Neural Dynamics of Label Understanding and Their Role in Attentional Selection and Distractor Inhibition in Children

A Dissertation Presented for the

Doctor of Philosophy

Degree

The University of Tennessee, Knoxville

Hollis Lee Ratliff Heim

May 2025

ACKNOWLEDGEMENTS

I want to first thank my advisor, Dr. Aaron Buss, for his constant mentorship. I am grateful for the freedom you gave me to explore ambitious questions, and your generosity of time and lab resources to allow me to accomplish my goals. I am also thankful to Dr. Caglar Tas, who helped me set up eye-tracking and deepened my understanding of visual attention. Thank you to Dr. David Sutterer, who helped me develop the EEG data collection and preprocessing code, and who generously allowed me to use gel, syringes, and EEG equipment from his lab for data collection. An additional thank-you to Drs. Greg Reynolds, Lowell Gaertner, and Lori Caudle for serving on my committee and giving me a well-rounded understanding of visual attention, EEG, and statistics. Further, I want to thank Connie Ogle for helping me with paperwork, cutting through all the red tape involved in getting a PhD.

I also want to thank members of my lab: Dr. Kara Lowery, Dr. Kaleb Kinder, Rachel Eddings, and Dr. Jessica Defenderfer, who offered deep mentorship in my first years as a graduate student. I want to thank Jes Parker, for helping set up eye-tracking for my study, and Jim Cooper, who helped in data collection and Alexis McCraw, who has been a wonderful collaborator and strong intellectual friend. I also want to acknowledge the undergraduate research assistants who made my dissertation possible: Sydney Thompson and Neekon Nejad. Without them, I could not have collected the data for this project or created the protocol for the EEG/fNIRS cap setup.

To my mother and father, Sunny Ratliff and Franklin Ratliff, thank you for the constant support and belief that I could accomplish great things if I set my mind to it. You have always encouraged me to think creatively, and those skills have carried me through my academic career. To my older sister, Kallie Bennett, thank you for our conversations and your perspective as a speech-therapist that helped enrich my dissertation. Thank you to my siblings Mary Kate Ratliff and Matthew Ratliff, for your love and devotion throughout my life.

Thank you to my mother-in-law, Dulcie Heim, and sister-in-law Emily Heim, for watching my kids so that I could write my dissertation. In addition, thank you to my friend, Devin King for her help in editing my dissertation.

To my husband, Andrew, thank you for the sacrifices you made to allow me to devote the necessary time to complete this dissertation. Without the daily intellectual conversations, daily laughs, and daily love that we share, this accomplishment would not have been possible. Thank you to my beautiful children: 3-year-old Arthur and 1-year-old Ava. You give me constant reasons to smile.

Lastly, I give all glory and honor to the Father, Son, and Holy Spirit, for the fortitude, humility, and diligence to complete this dissertation.

This work is dedicated to my children: Arthur, Ava, and the one on the way. You make my academic pursuits mean something.

ABSTRACT

Previous research focuses on the ability of label representations to guide attention towards relevant features. However, the relationship between label representation and the ability to inhibit irrelevant information is less understood. The current study aims to assess how label representations can not only guide attention but suppress irrelevant distractors. To accomplish this, 36 8- to 10-year-olds performed the Dimensional Label Understanding (DLU) tasks and the additional singleton (AS) paradigm while fNIRS and EEG were measured. The AS paradigm allows for control of the saliency of distractors in the tasks by modifying the salience of distractors in different conditions. The current study seeks to analyze whether neural correlates of DLU predict individual differences in children's reaction time during the AS paradigm. It was found that participants who were not distracted by irrelevant information in the AS paradigm activated the inferior frontal cortex and angular gyrus during the AS paradigm. In addition, these participants activated the right lateralized frontal-parietal network involved in bottom-up attentional networks during the DLU tasks, suggesting that children who have bottom-up label processing are better able to suppress irrelevant information. These results highlight the effectiveness of the attentional strategy of having a strong representation of features in order to better find targets and inhibit irrelevant information.

TABLE OF CONTENTS

LIST OF TABLES

LIST OF FIGURES

CHAPTER ONE: Introduction

Background

Previous research focused on the ability of label understanding to guide attention, demonstrating that an increase in dimensional label understanding (DLU) can help selectively attend to features of an object (Heim et al., 2023; McCraw et al., 2024). For example, using the feature label, “red” can help guide an observer’s attention to selectively attend towards red apples at the grocery store. Other work in this area has shown that using labels increases performance in visual search tasks (Pickron et al., 2018; Vales & Smith, 2015). However, this literature has not directly explored how label understanding might aid in inhibiting irrelevant information. In the grocery store example, using the feature label, “red” may help an observer ignore irrelevant information such as the yellowness of a banana. In visual search tasks, an observer must search for a target while inhibiting attention towards distractors. When exploring the impact of label understanding, it is difficult to differentiate the constructs of attentional selection and inhibitory control. As such, the current study seeks to understand how label understanding, and the inhibition of distractors interact to aid in target selection.

To address this research question, the additional singleton (AS) paradigm, which can control salience of the distractors, was utilized. (Theeuwes, 1992). In the AS paradigm, participants are asked to find a target among distractors (**Figure 1**). The AS paradigm has two conditions: AS Absent and AS Present. In the AS Absent Condition, the target (e.g., green diamond) and distractors (e.g., green circle) are all the same color.

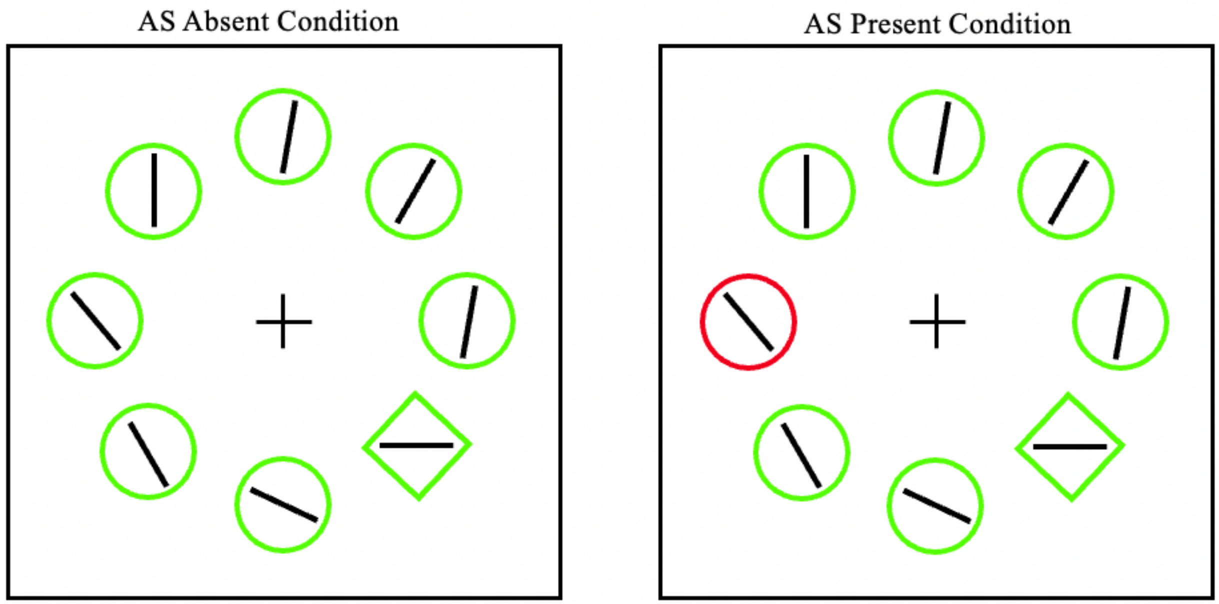

Figure 1. Stimuli of the additional singleton (AS) paradigm from Theeuwes (1992). Participants search for a target, a green diamond among circles and respond to the orientation of the target (vertical vs horizontal). In the AS Absent Condition, all distractors and targets are the same color. In the AS Present Condition, one of the distractors is a different color than the target.

However, in the AS Present Condition, there is one distractor that is a different color (e.g., red circle). This color singleton distractor holds irrelevant information for the visual search as the observer is searching for a shape. Previous research has shown that the presence of the different-colored distractor in the AS Present Condition increases reaction time (RT) by capturing the participant's attention (de Fockert et al., 2004; Theeuwes, 2004). The nature of the AS paradigm allows for the experimenter to assess the effect of an irrelevant distractor on visual search performance. As a result, we can assess if label understanding aids in the ability to not only find a target but inhibit irrelevant information in a visual search.

The Developmental Relationship Between Dimensional Label Understanding and Attention

Label representations involve more than just learning vocabulary, but also include learning dimensional labels. Sandhofer & Smith (1999) defined dimensional labels as a system of mappings involving word-word mappings (e.g., learning that the label, "color" is associated with, "red" and "blue"), word-property mappings (e.g., "Show me the red one"), and property-property mappings (e.g., matching colors and shapes). Children learn word-word mappings first, followed by word-property mapping, and then eventually combine those two skills to perform property-property mapping in which objects are matched based on a specific feature (Sandhofer & Smith, 1999). In this theoretical lens, children must first learn a series of color labels in order to guide their attention to the relevant dimension, allowing them to selectively attend to the target object. Indeed, Lowery et al. (2022) found that neural mechanisms of the Label Production task (word-word mapping) at 33-months predicted dimensional attention ability, the ability to selectively attend to features of an object, at 45-months. Taken together, these findings demonstrate that dimensional label understanding, specifically the production of labels, predicts children's ability in dimensional attention tasks.

A further study by McCraw et al. (2024) explored whether label understanding predicted executive function longitudinally from 30- to 54- months old using fNIRS. Children performed Label Production and Comprehension tasks at 30-months and a battery of executive function tasks at 54-months, that included the Dimensional Change Card Sort Task (DCCS; **Figure 2a**). In the DCCS task, children are shown two target cards (e.g., a purple house and a yellow fish) and are asked to sort cards (e.g., a yellow house and a purple fish) by either shape or color. After sorting by one feature (in this instance color) for several trials, children are then told to switch and sort by the other feature (shape). Most 3-year-old children perseverate, continuing to sort by the original dimension, whereas 5-year-old children can switch and sort by the new dimension (Zelazo, 2006). In McCraw et al. (2024), it was found that neural mechanisms of the Label Production task at 30-months was related to high performance in the DCCS at 54-months, suggesting that individual differences in brain activation while children are labeling colors and shapes can predict flexible attention later in development.

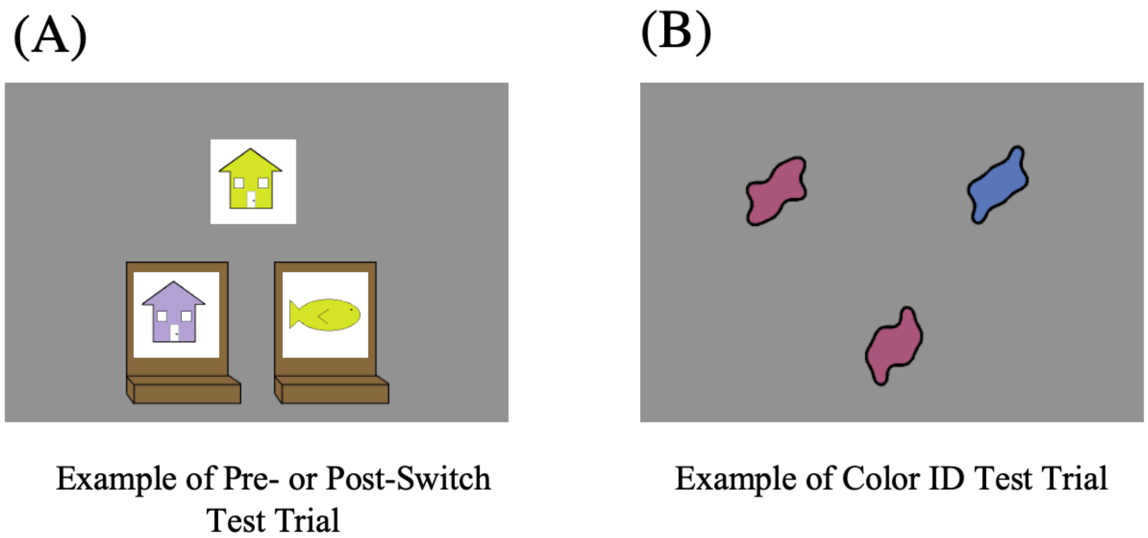

Figure 2. Stimuli for the Dimensional Change Card Sort (DCCS) task and the triad classification (TC) task (A) Sample of a DCCS trial. Children are first asked to sort by one dimension (e.g., color) and then switch and sort by the opposite dimension (e.g., shape). Most 3-year-old children perseverate and continue to sort by the original dimension (e.g., color) whereas 5-year-old children can switch and sort by the new dimension (e.g., shape; Zelazo, 2006). (B) Sample of a TC trial. One of the objects is exactly similar on one dimension (e.g., pink) but completely opposite on the other dimension (e.g., 180° different shape). The other object is more holistically similar to the reference object (90° color and 90° shape). There is a developmental shift seen in this task such that 3-year-olds tend to pick the object that is more holistically similar to the reference object while 4-year-olds tend to pick the object that shares a feature (e.g. same color; Smith & Kemler, 1977).

Heim et al. (2023) also explored the relationship between neural activation during Production and Comprehension Tasks and dimensional attention in preschool children. One of the dimensional attention tasks performed in this study was the Triad Classification (TC) task. In this task, children are presented with three odd shapes (**Figure 2b**). The experimenter then asks the children, "which of these two is like this one" and points at the reference shape. One of the choices is the exact same on one dimension (e.g., same color as the reference shape), but markedly different on the other dimension (180° different shape as the reference shape). This option is referred to as the *identity match*. The other option is more holistically similar to the reference object on both feature dimensions. This option is referred to as the *holistic match*. There is a developmental shift seen in this task such that 3-year-olds tend to pick the object that is more holistically similar to the reference object while 4-year-olds tend to pick the object that shares one feature such as the same color (Smith & Kemler, 1977). The TC task measures children's ability to selectively attend to features of an object. For example, if a child can selectively attend to color, they should more easily choose the identity match instead of holistically processing both dimensions. Heim et al. (2023) reported that children who chose the *identity match* in the TC task activated the parietal cortex during the Label Production and Comprehension task, indicating that children who are more able to selectively attend have stronger activation in the parietal lobe during the DLU tasks. These findings showcase the importance of label understanding as a mechanism for selective attention, in that that labels can guide attention towards relevant features of an object.

Label Representations Guide Attention

Children who have better label representations may use label representations to guide attention to the relevant dimensions in the task. Buss & Nikam (2020) found that verbally prompting specific labels helped children flexibly shift their attention. In this experiment, children were split into two groups: one group was given DCCS instructions that involved the dimension and feature label of the object (e.g. star or blue), the second group was given DCCS instructions that involved the dimension label (e.g. shape or color). Those in the second group who were given only the dimension labels perseverated at a higher rate when compared to those in the first group who were given both dimension labels and feature labels (Buss & Nikam, 2020). These results suggest that the understanding of visual labels can aid in performance during the DCCS, allowing for shifting of attention to relevant features in the DCCS.

In addition to dimensional attention, labels can aid in visual search by guiding working memory to find a target successfully in a visual search paradigm (Huettig et al., 2011). Vales & Smith (2015) showed that labels aided in visual search in preschool aged children. Merely hearing the name of the target helped preschoolers locate the target faster in a visual search task. Further research conducted by Mani et al., (2013) found that children were quicker to find a target (e.g., yellow cup) when given a color matching label (e.g., banana) when compared with an unrelated label (e.g. house). Further, children were able to find a target even faster when they were provided with a semantically related word, for example, participants were faster to find a cookie if given the label “banana” (Mani et al., 2013). In a study by Pickron et al. (2018), 6-month-old infants were trained for 3 months on either category labels, specific labels or no labels at all. It was found that the infants who were trained on specific labels showed an increase in visual attention seen by a larger Nc ERP component, an ERP marker for attention in infancy. These results further demonstrate that labels can have a direct impact on visual search ability. The research discussed thus far analyzes the role of label understanding on guiding attention towards relevant information in a task. However, label understanding also has the potential to suppress aspects of the environment that are salient, but irrelevant.

Dimensional Labels as a mechanism of inhibitory control

Research has shown that inhibition ability can aid in grammar, in that inhibitory control is a better predictor of grammatical ability in preschool aged children compared to vocabulary and age (Ibbotson & Kearvell-White, 2020). An explanation for this is the need to inhibit irrelevant competition when using the correct tenses. While these findings suggest that inhibition ability can aid in language understanding, other studies have found that labels can aid in a motor inhibition task. For example, a study exploring inhibitory control tasks in children between the ages of 7- and 13- years old found that using labels significantly lowered reaction time for younger children in a stop-signal task, which assesses children’s ability to inhibit a response to a stimulus (Kray et al., 2009). These results suggest that labels can aid in suppressing a motor response, however, other work must be examined to fully understand the role of inhibitory control and language in guiding attention.

One recent study by Chabal et al. (2021) explored the role of phonetic competition in visual search, and whether vocabulary ability or inhibitory control impacted 8- to 12- year old’s fixation duration to distractors. In this study, children were shown a target appearing in the middle of the screen followed by a display of four objects. One of the conditions consisted of a distractor that shared phonemes with the target. It was found that children fixated significantly longer on the similar-phoneme distractor (e.g., drum with dress) when the child scored high in language ability but low in inhibitory control. In contrast, children with high language ability and high inhibitory control demonstrated no significant differences in fixation between the conditions. It seems that children with higher language ability were more likely to be affected by a language-related distractor. However, this effect was mitigated by inhibitory control ability. Although Chabal et al. (2021) briefly mentions the relationship between children’s labels and inhibitory control, the study is primarily focused on whether language ability can help inhibit relevant information (i.e. the distractor has shared linguistic information with the target). By contrast, the current study will employ a distractor that holds irrelevant information to the target, to determine whether language ability also inhibits irrelevant information.

Developmental Markers of the Additional Singleton Paradigm

The current study can answer the question of the relationship between label understanding and inhibitory control by turning to the AS paradigm (Theeuwes, 1992). When looking at this behavioral effect in children, research has indicated that children are slower in both the AS Present and AS Absent Condition compared to adults (Blakley et al., 2022; Sun et al., 2018). Despite holding irrelevant information, the color singleton distractor in the AS Present condition captures the observer's attention and requires inhibitory control to suppress the distractors to find the target.

One study using fMRI has demonstrated that the singleton distractor is associated with activity in the frontal and parietal cortex in adults (de Fockert et al., 2004). Additionally, reaction time was negatively correlated with frontal cortex activity during the singleton distractor condition, suggesting that the frontal cortex is involved in inhibiting the singleton distractor (Lavie & de Fockert, 2006; de Fockert & Theeuwes, 2012). Although no fMRI research has been conducted on children using the AS paradigm, research into the neural mechanisms of attentional selection and inhibition in early childhood has shown that measures of inhibitory control, such as the Go/NoGo task, involve activation in the dorsal and ventro-lateral prefrontal cortex as well as the parietal cortex (Fiske & Holmboe, 2019). One study that looked at neural activation during fMRI while adults and children completed a Go-No Go task found that children had stronger activation in prefrontal and parietal regions during a response inhibition task compared to adults (Durston et al., 2002). This suggests that children require more cognitive resources to successfully inhibit distractors compared to adults. Other research has demonstrated that adolescent children activate the dorsal anterior cingulate cortex, dorsolateral prefrontal cortex, and fronto-striatal regions during inhibitory control tasks (Jaeger, 2013). These results highlight the developmental shifts and neural nuances seen in inhibitory control.

EEG research on children has shown developmental shifts in attentional selection and inhibition. During visual search, there is and ERP component appearing around 200ms after stimulus presentation known as the N2pc component, which is a marker for selective attention and target selection (Couperus & Quirk, 2015; Rashal et al., 2022; Sun et al., 2018). Evidence has shown that children exhibit a similar but smaller N2pc pattern in visual search tasks compared to adults (Couperus & Quirk, 2015; Sun et al., 2018). Liesefeld et al. (2017) explored not only the N2pc component, but the Distractor Positivity (P_D) component, a positive increase in activation contralateral to the distractor, interpreted as an active suppression mechanism. This study demonstrated that a distractor in an AS paradigm was suppressed by evidence of a N2pc followed by a P_D component (Liesefeld et al., 2017). Another study found individual differences in the P_D depending on children's performance such that children who performed poorly in a visual search task exhibited a high P_D of the distractor whereas children who performed well had a smaller, more adult-like P_D (Sun et al., 2018). Taken together, these results suggest a developmental shift between 8- and 9- years old in which the N2pc component starts to take a similar form as adults (Couperus & Quirk, 2015; Deveney et al., 2019; Sun et al., 2018; Turoman et al., 2021). In addition, these results show that well-performing children in the AS Paradigm display more adult-like suppression of the distractor but are less effective at attentional selection of the target compared to adults.

As seen in the N2Pc and P_D ERP research, there is a neural shift that occurs after 8-years-old in children's ability to attend to a target and inhibit distractors, although the explanation for this shift is yet to be explained. The shift could be a result of a difference in attentional strategy between adults and children, as the N2pc component is thought to represent both top-down and bottom-up attentional processes (Hickey et al., 2006; Liu et al., 2016). However, exploring the potential of label understanding as a mechanism for this developmental shift in inhibitory control may provide a deeper explanation of the mechanism involved, extending our understanding beyond age-maturation. The current study targets the developmental age range of 8- to 10-years-old in order to uncover the relationship between a child's label understanding and their ability to suppress irrelevant information. If Dimensional Label Understanding impacts inhibitory control, the current study will show that dimensional labels will not only aid in guiding attention towards relevant information, but also aid in suppressing irrelevant information.

Top-Down and Bottom-Up Attention as Attentional Strategies

In the AS paradigm, the singleton distractor captures the observer's attention, and therefore is indicative of bottom-up/stimulus driven attention, whereas the act of inhibiting the distractor displays top-down attention, actively controlling attention to find the target (Theeuwes, 2010). However, depending on the task demands, observers display different attentional strategies to find the target more efficiently. For example, it was found that if the AS paradigm was altered such that the observer was looking for a target among distractors of different shapes, and one distractor of a different color, the observer was no longer captured by the additional singleton distractor (Bacon & Egeth, 1994). These results suggest that observers will switch strategies from a "singleton-detector mode" to a "feature search mode" in order to find the target more efficiently. Similarly, research has been done into learning strategies in the AS paradigm such that participants can learn to suppress the color singleton over time, if they realize the information is irrelevant (Gaspelin et al., 2015; Vatterott et al., 2018).

Research into the N2pc and P_D components during the AS paradigm for adults have revealed a learned suppression of the additional singleton distractor characterized by the existence of the P_D component for highly salient distractors, suggesting that observers learned to suppress the singleton distractor (Gaspelin & Luck, 2018; Stilwell et al., 2022). Sun et al., 2018 did not specifically look at learned suppression as a strategy for children, however, they found that children did display a similar P_D component as adults, suggesting that children may be displaying a similar strategy of actively suppressing the singleton distractor. However, the mechanism of how children develop the attentional strategy of learned suppression of irrelevant information has not been explored. Thus, the current study seeks to assess if children's understanding of labels aids in the inhibition of salient distractor information during the AS paradigm.

Present Study

The current study assesses whether the individual differences in neural activation during DLU tasks and the AS paradigm predict children's ability to inhibit distractors and find a target in a visual search task. To accomplish this, fNIRS data was collected on 8- to 10- year-olds during Production and Comprehension label understanding tasks and the AS paradigm. In this study, two brain-behavioral analysis were conducted: 1) neural activation during the AS paradigm predicting RT differences during the AS paradigm and 2) neural activation during the DLU tasks predicting RT differences during the AS paradigm. For the first brain-behavioral analysis looking at neural activation during the AS paradigm, we predict that there will be differences in frontal cortex activation for children who have lower distractibility during the AS paradigm, expanding on the results found in Lavie & de Fockert (2006). The second brain-behavioral analysis will test whether there are neural activation patterns during DLU that can predict level of distractibility during the AS paradigm. If neural activation observed during DLU tasks predicts children's ability to inhibit distracting information, then the current study will demonstrate that there are neural patterns during DLU that not only aid in attention towards relevant features, but also in suppressing irrelevant features.

Measurements

Children completed the Production and Comprehension label understanding tasks. We predict that children will reach ceiling behaviorally for the label understanding tasks, because typically developing children have practiced and internalized shape and color labels. However, we expect to observe individual variability in neural activation based on extracted hemoglobin values during the label understanding tasks that predict differences in performance during the AS paradigm. Therefore, for the DLU tasks, oxygenated hemoglobin (HbO) and deoxygenated hemoglobin (HbR) were analyzed using Image Based Analysis over frontal and parietal regions of the brain. Activation is defined as an increase in HbO coupled with a decrease in HbR reflecting neurovascular coupling (Kinder et al., 2022; Tachtsidis & Scholkmann, 2016).

In addition to the DLU tasks, children completed the AS paradigm. The AS paradigm consists of two conditions: AS Present and AS Absent. In the AS Absent Condition, the trials are a simple visual search task in which the participant is told to search for a circle among diamonds. In the AS Present Condition, the trials are the same as the AS Absent Condition with one difference: one of the distractors is a different color. The AS Present Condition presents a greater amount of distractibility due to the different-colored singleton capturing the child's attention. As a result, the observer must inhibit attention towards the irrelevant distractor to find the target.

Aims and Hypotheses

The current study first aims to replicate adult AS paradigm behavioral results showing that the AS Present Condition causes slower reaction times and lower accuracy in children (Fockert et al., 2004; Theeuwes, 2004). This replication establishes that adding the singleton distractor requires more inhibitory control for the participant. In addition, we expect to find that older children perform better (faster reaction time, higher accuracy) on the AS paradigm compared to younger participants.

The second aim of this study is to analyze the neural mechanisms of the AS paradigm in children and establish if individual differences in RT can predict brain activation during the AS Absent and AS Present Conditions. We expect to see that children activate the frontal and parietal cortex during the AS Present condition, mirroring results found in adults (Lavie & de Fockert, 2006; de Fockert & Theeuwes, 2012). In addition, we expect to find that participants who had lower distractibility (HbDiff) will show higher activation in the inferior frontal cortex compared to participants with higher distractibility (HbDiff), reflecting participant's effectiveness of inhibiting the irrelevant distractor.

Finally, the current study explores whether individual differences in neural activation during the DLU tasks predicts AS performance for each condition. We expect to see that parietal lobe activation (Heim et al., 2023) and frontal cortex activation (Lowrey et al., 2022; McCraw et al., 2023) during Label Production and Comprehension tasks predict RT during the AS Conditions. The current study will explore whether neural activation during Production and Comprehension tasks will reveal that higher-order processing for labels impacts the level of distractibility (RTDiff) in participants. If neural activation during the DLU tasks predicts participants with low distractibility, then we can reveal the nature of how dimensional label understanding can aid in the inhibition of irrelevant information.

CHAPTER TWO:

MATERIALS AND METHODS

Sample

38 children between the ages of 8- and 10-years old were recruited from the Knoxville, TN area through a database maintained by the Child Development Research Group of the University of Tennessee, Knoxville. A total of 36 participants were included in the analysis (M_{age}=8.99 years, N_{male}=20). One participant was excluded due to a parent-reported autism spectrum disorder (ASD) diagnosis. In addition, one participant was excluded due to inability to demonstrate understanding of the task instructions.

Apparatus

The current study measured fNIRS, EEG, and eye tracking while children completed the AS paradigm as well as the Dimensional Label Production and Comprehension Tasks.

EEG/fNIRS Setup

The study utilized a Brain Products actiCHamp system of 32 electrodes mounted on an elastic cap using the international 10-20 sites (O2, Oz, O1, P8, P4, Pz, P3, P7, PO8, PO4, POz, PO3, PO7, T8, C4, Cz, C3, T7, FC6, FC5, F8, F4, Fp1, Fz, Fp2, F3, and F7). Four additional electrodes with stickers were placed on the left and right mastoids and in the corners of the left and right eyes to measure eye movements using Electrooculugram (EOG). The left mastoid served as the reference during acquisition. EEG data was preprocessed using eeglab in MATLAB (Delorme & Makeig, 2004).

The fNIRS lights and detectors configuration consisted of 8 sources and 16 detectors configured on the bilateral frontal and bilateral parietal cortex for a total of 24 channels. The lights and detectors were placed in between EEG electrodes so as not to interfere with the electrode signal (**Figure 3**). A digitization of the fNIRS probe was made using a Polhemus motion tracking system marking the probe's location relative to landmarks (nasion, inion, left tragus, right tragus, and vertex). fNIRS data was collected at 25 Hz using a TechEn CW7 system with wavelengths of 830 nm and 690 nm. fNIRS data was processed using Forbes et al., (2022) MRI-NIRS Pipeline, which involves using fNIRS analysis software Homer 2 (Huppert et al., 2009), fNIRS preprocessing toolbox NeuroDOT (Eggebrecht & Culver, 2019), and fMRI analysis software AFNI (Cox, 1996).

An Eyelink 1000 Plus eye tracker sampling at 1000 Hz was used to monitor eye movements during the AS paradigm. A chinrest ensured a viewing distance of 92 cm. A target sticker was placed over the right eye of the participant for calibration.

Additional Singleton Paradigm

In the AS paradigm, participants searched for a circle among 7 distractor diamonds (**Figure 4**). Participants were instructed to look at a fixation cross in the center of the screen and press a button indicating whether the circle appears above in the upper half of the screen or below in the lower half of the screen. Participants pressed the left blue button if the circle appeared on the upper half of the screen and pressed the right yellow button if the circle appeared on the bottom half of the screen. Participants were

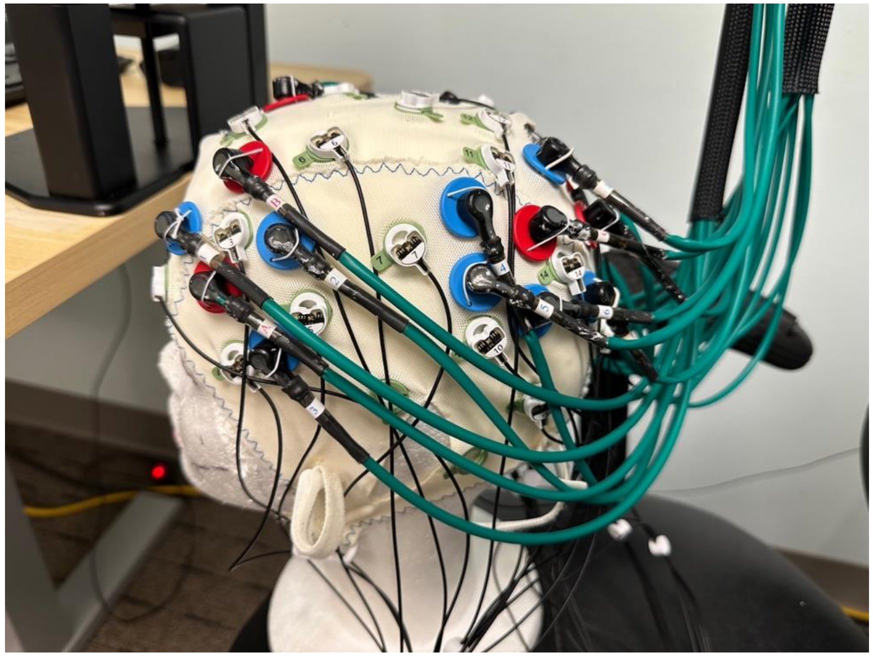

Figure 3. Photo of the fNIRS-EEG cap used in the current study. EEG electrodes were placed using the international 10-20 sites. The fNIRS lights (red grommets) and detectors (blue grommets) were positioned as to not interfere with the EEG electrodes. fNIRS probe was configured to measure frontal and parietal regions.

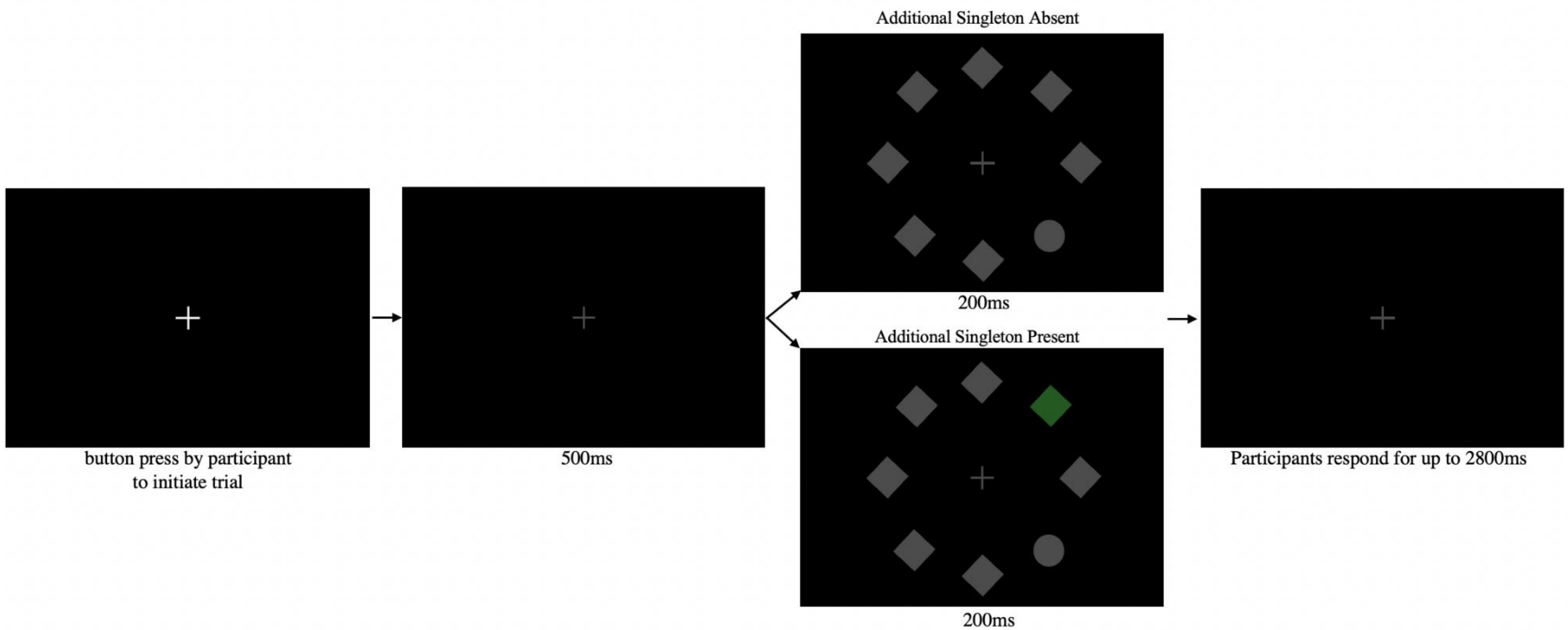

Figure 4. Additional singleton paradigm stimuli for the current study. The white fixation cross appears as a marker for the participant to initiate the trial. Then, 500ms of a gray fixation cross appears before trial onset. The trial display appears for 200ms and then changes to a gray fixation cross awaiting participant's button press.

instructed to not move their eyes when the search display appeared. Additionally, the experimenter coached the participant on the eye tracking system to ensure that they did not fixate on the target or button box when they made their response.

There were two conditions in the AS paradigm: AS Absent and AS Present. In the AS Absent condition, participants searched for a gray circle among 7 gray diamonds, presented every 45° with a radius of 25% of the y-axis screen pixels. In the AS Present condition, participants searched for a gray circle among 6 gray diamonds and one additional singleton diamond of a different color. The color singleton distractor diamond appeared either red (RGB: 168, 20,10) or green (RGB: 15,88,30). All colors used in the task were controlled for luminance (17.6 cd/m^3). Condition (AS Absent, AS Present) and color for the singleton distractor (red, green) were randomized throughout the task. A total of 400 trials were presented to each participant, 200 trials per condition (AS Absent, AS Present). For the AS Present condition, 100 trials had a red color singleton, and 100 trials had a green color singleton.

Each trial began with a white fixation cross (80 pixels in length, 4 pixels in thickness) in the middle of the screen that remained until the participant made a button press to start the trial. When the trial was initiated, the centered fixation cross changed to gray and was presented for 500 ms, after which, the stimulus array appeared for 200 ms followed by a blank screen with a fixation cross for up to 2800 ms, during which participants made their responses. If participants did not respond in 2800 ms, the trial was marked as a bad reaction time, and the next trial started. The average rate of bad RT was

8.01% of trials for the AS Absent Condition and 7.95% of trials for the AS Present Condition. There was no relationship between bad RT rates and Age, $r(36)=-.21$, $p=.23$. Trial onset times were synchronized with fNIRS and EEG data collection. All tasks were optimized for functional neuroimaging by jittering the inter-trial interval (i.e., randomly varying the time between trials) at either 1, 3, or 5 seconds with additional time allotted to orient the child toward the screen and prepare for the next trial.

Dimensional Label Understanding tasks

Participants completed four tasks with 12 trials each: Color Production, Color Comprehension, Shape Production, and Shape Comprehension while fNIRS and EEG data collected (**Figure 5**). The task order was randomized for each participant. The Production task involved showing a child a single object and asking them to report the object's shape or color verbally. The Comprehension tasks involved presenting an array of 6 objects that all have different shapes and colors. Participants were asked to find an object with a specific feature label by indicating their response with a mouse. All tasks were optimized for functional neuroimaging by jittering the inter-trial interval at either 1, 3, or 5 seconds with additional time allowed to orient the child toward the screen and prepare for the next trial.

Procedure

The first part of a study session consisted of 30-40 minutes of setup. Participants sat in a chair facing a computer monitor. A booster seat was provided if the participant was too short. During setup, participants watched a movie of their choice on the computer

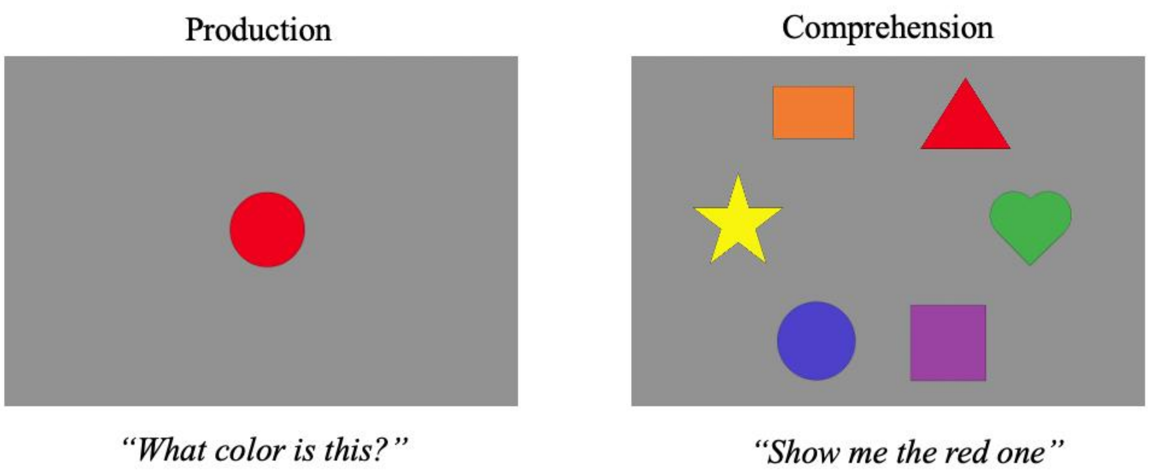

Figure 5. Dimensional Label Understanding Task. The Production task consisted of participants making a verbal response to "What color/shape is this?". The Comprehension task consisted of participants using a mouse to find either a color or shape.

monitor. The fNIRS/EEG cap was measured on the participant's head such that the Cz electrode was situated at the centerpoint of the scalp. Next, a digitization of the fNIRS probe was made using a Polhemus motion tracking system. A quality check was then performed on the fNIRS system and lights and detectors were adjusted if necessary. After setup was finished, Participants completed the first half of the AS paradigm. They then moved onto the DLU tasks. When these were completed, participants began the second half of the AS paradigm. The tasks took approximately 45-60 minutes to complete total, Including built in breaks.

Additional Singleton Behavioral Data Preprocessing

Both accuracy and RT were collected during the AS paradigm. Because RT is typically right skewed, the data is subject to potential outliers. Therefore, the median reaction time (RT) for correct trials was extracted to better reflect each participant's RT. Normality tests were conduction on the distribution of median reaction time before using these scores in parametric tests. A difference score of AS Present RT - AS Absent RT was calculated to create a variable measuring distractibility (RTDiff). Higher scores represent participants who had slower RT in the AS Present Condition, who show a higher distractibility compared to participants with low scores.

EEG Preprocessing

EEG data was re-referenced and segmented in 2s epochs around the trial onset (-800ms:1250ms). Artifact rejection for high frequency noise, drift, blocking, channel dropout, blinking and eye movements were conducted for each participant.

The majority of participants were unable to avoid moving their eyes during the tasks. Only 19% (*N*=7) of participants had enough usable EEG AS trials. Of the 7 usable participants, the average artifact rejection rate was 39.5% of trials. In addition, 13 participants did not complete the full 400 trials of the AS paradigm due to fatigue (*N*=6), session timing issues (*N*=5), or EEG technical issues (*N*=2) with an average completion of 323 trials. Because of these complications, the present study focuses specifically on the analysis of behavioral and fNIRS data.

fNIRS Preprocessing

To create a sensitivity profile for each participant, we used Colin27 atlas (Collins et al., 1998) to register the fNIRS data onto a 3d headspace. Monte-Carlo simulations launched 10,000,000 photons for each wavelength (690nm, 830nm) and channel on the fNIRS probe (**Figure 6a**). Sensitivity profiles for each channel were thresholded at 0.0001, filtering out low sensitivity, and combined to create participant-specific masks. These masks reflect the cortical volume of all recording fNIRS channels for each participant. Analysis was then conducted within voxels (i.e., a 3d pixel representing a small cubic area of the brain) where at least 60% of participants contributed data (**Figure 6b**).

We used EasyNIRS Homer2 software to both calculate the mean baseline and transform the data into a measure of optical density (Huppert et al., 2009). An interquartile range of .72 with a wavelet-based motion artifact removal tool within EasyNIRS was applied to correct motion artifacts. The data were then band-pass filtered

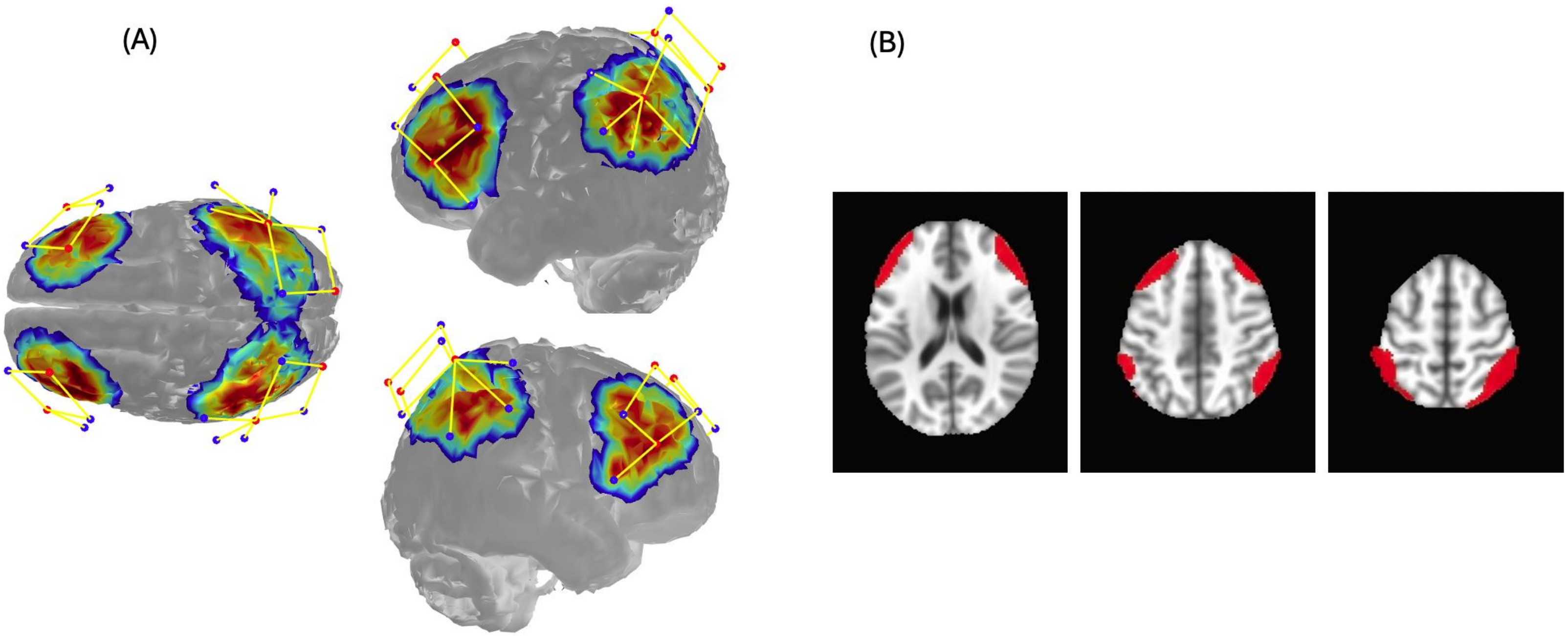

Figure 6. Brain regions measured. (A) Sensitivity profile created by launching 10 million photons for each wavelength and channel. This is a sample from participant S104. (B) Mask used for analysis in which 60% of participants contributed data.

(high-pass filter = .01, low-pass filter = .50) and converted to absolute concentration values using the modified Beer-Lambert Law (Boas et al., 2001) and the known extinction coefficients of HbO and HbR with differential and partial pathlength factor values of 6.0.

Next, tools in the NeuroDOT toolbox (Eggebrecht & Culver, 2019) were used to project the channel-based fNIRS data onto each sensitivity profile. Once this was completed, a global signal regression was carried out on optical density data to remove global changes throughout the measurements and to retain signals specific to each channel (Murphy & Fox, 2017). The sensitivity matrix was then inverted, to transfer the fNIRS data to a brain image. However, the inversion generates an underspecified solution (i.e., there are far more voxels measured than fNIRS channels, with infinite possible combinations of voxel activations). This issue is solved with the Tikhonov regularization method, adding constraints to the solution by creating a Moore-Penrose generalized inverse (i.e. λ=.01 Tikhonov regularized and $\lambda 2$ = .1 spatially variant regularization). This step optimized fNIRS spatial correspondence with fMRI data, which allows for the fNIRS data to be analyzed as fMRI data (Wheelock et al., 2019).

Image-Based Analysis

The image-based analysis consisted of two separate general linear models. The first model estimated the amplitude of hemodynamic responses for the two conditions of the AS paradigm (AS Absent, AS Present). The second model estimated the amplitude of hemodynamic responses for each DLU task (Color Production, Color Comprehension, Shape Production, Shape Comprehension). For both models, using the timing for each trial, a 10 second boxcar function was aligned for each trial onset. The GLM estimated the amplitude of change for both HbO and HbR within each voxel during each condition. Data was then transformed to a common group space (i.e. aligned to a shared brain map). After the data was transformed to a common group space, 3dMVM in AFNI (Chen et al., 2014) assessed factors of interest. 3cluststim (Cox et al., 2017) corrected for family-wise error with voxel-wise alpha <.05 and cluster-wise alpha < .05. HbO and HbR concentrations were then extracted to better visualize the interactions.

CHAPTER THREE:

RESULTS

Behavioral Results

Additional Singleton Performance

A paired samples *t*-test was performed to assess if there were RT differences between AS Absent versus AS Present Condition. It was found that there was a significant difference between the conditions such that the AS Present Condition (*M*=733ms, *SD*=311) had slower RT compared to the AS Absent Condition (*M*=705ms, *SD*=297), *t*(35)=2.61, *p*=.013, *d*=.43 (**Figure 7a**).

A Wilcoxon signed-rank test was performed to assess if there were significant differences in AS Accuracy between conditions. It was found that there were no significant differences in performance between AS Present (*Mdn*=.94, *M*=.87) and AS Absent conditions (*Mdn*=.95, *M*=.90), *W*(36)=-1.30, *p*=.196 (**Figure 7b**).

Age Predicting Additional Singleton Performance

A repeated measures ANOVA was conducted to determine the effect of condition (AS Absent, AS Present) on reaction time with age as a covariate. There was a main effect of condition, controlling for age, such that the AS Present condition (*M*=733, *SD*=311) had slower RT compared to the AS Absent condition (*M*=705, *SD*=297), *F*(1,34)=8.55, *p*=.006, ηp^2=.20. In addition, there was a significant interaction between Age and Condition, *F*(1,34)=7.36, *p*=.010, ηp^2=.18. Simple slope analysis was used to assess the relationship between AS condition and Age. It was found that in the AS

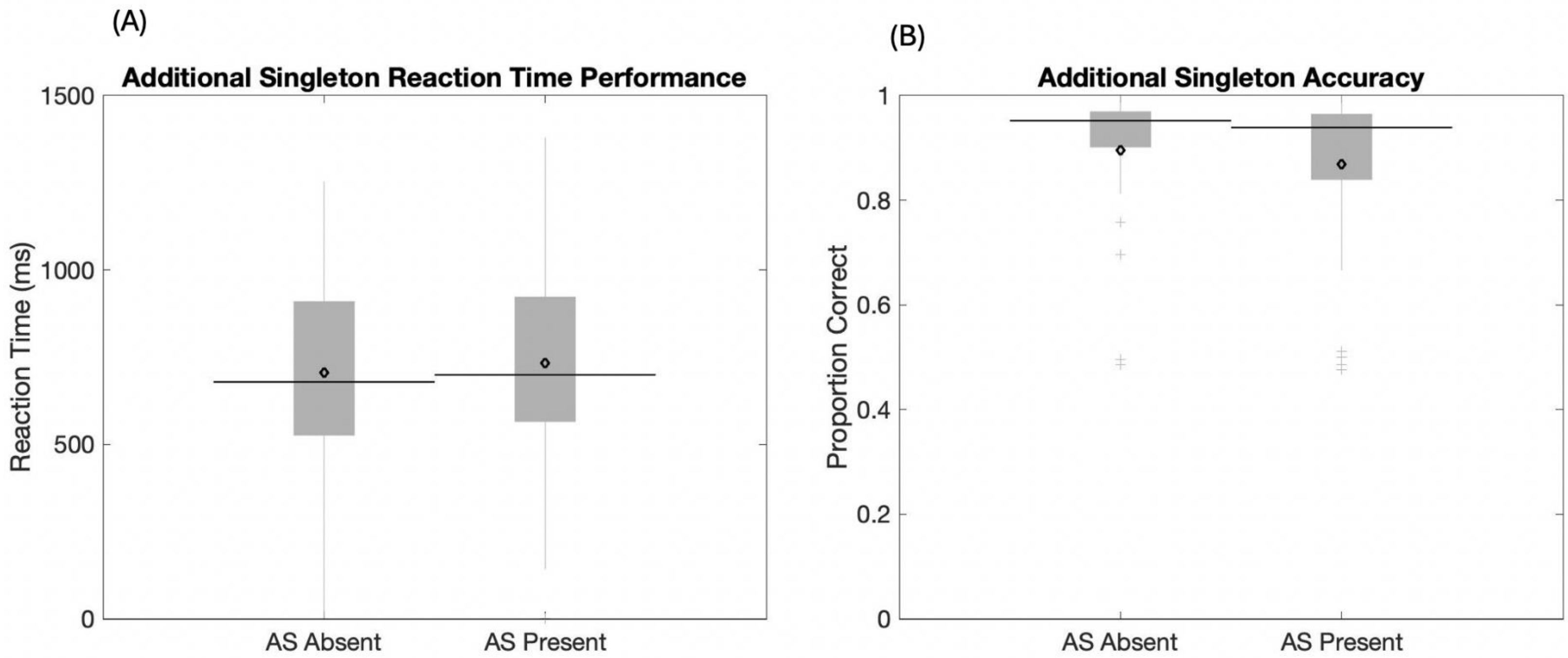

Figure 7. Behavioral results for performance on the additional singleton paradigm. (A) Reaction Time Performance for each condition in the AS Paradigm. AS Present had a slower reaction time compared to AS Absent, *p*=.013. (B) Accuracy for the Additional Singleton Paradigm. There were no significant differences in accuracy between AS Absent and AS Present.

Absent Condition, Age predicts reaction time such that as age increases, RT decreases, p=0.031. In addition, in the AS Present Condition, Age predicts reaction time such that as age increases, RT decreases, p=0.009 (**Table 1**). Further simple slope analysis was used to predict the estimated marginal means in order to compare the AS Condition RT for mean age (*Age*=8.99), one standard deviation below the mean age (*Age*=8.30) and one standard deviation above the mean (*Age*= 9.70). For the younger children (*Age*=8.30), RT was slower for the AS Present Condition (M=867ms, SE=680) compared to the AS Absent Condition (M=812ms, SE=670), p<.001 ηp^2=.31. For the mean-aged children (*Age*=8.99), RT was slower for the AS Present Condition (M=733ms, SE=48) compared to the AS Absent Condition (M=705ms, SE=47), p=.008, ηp^2=.19. However, for the older children (*Age*= 9.70), there were no observed differences in RT between the AS Present Condition (M=599ms, SE=68) and the AS Absent Condition (M=598ms, SE=67), p=.957, ηp^2=0.00 (**Figure 8**).

Dimensional Label Understanding Task Performance

As expected, in each DLU task, accuracy was at ceiling for all participants: Color Production (M=.99, SD=.02), Color Comprehension (M=1.00, SD=.01), Shape Production (M=.99, SD=.04), and Shape Comprehension (M=.98, SD=.04).

Exploring the Brain-Behavior Relationship of the Additional Singleton Paradigm

To explore the neural differences between the AS Present and AS Absent conditions and whether those differences can be predicted by distractibility (RTDiff), a 3dMVM (a mixed effects ANOVA) in AFNI (Chen et al., 2014) was conducted by

Table 1. Parameter Estimates predicting Reaction Time (ms) for Age x AS Condition

Parameter	***b***	***SE b***	***t***	***p***	**95% CI**
Intercept	2083.73	612.50	3.40	.002	[838.99 3328.47]
Age x AS Absent	-153.17	67.86	-2.26	.031	[-297.08 -15.26]
Intercept	2455.66	621.69	3.95	<.001	[1192.22 3719.09]
Age x AS Present	-191.43	68.88	-2.78	.009	[-331.41 -51.45]

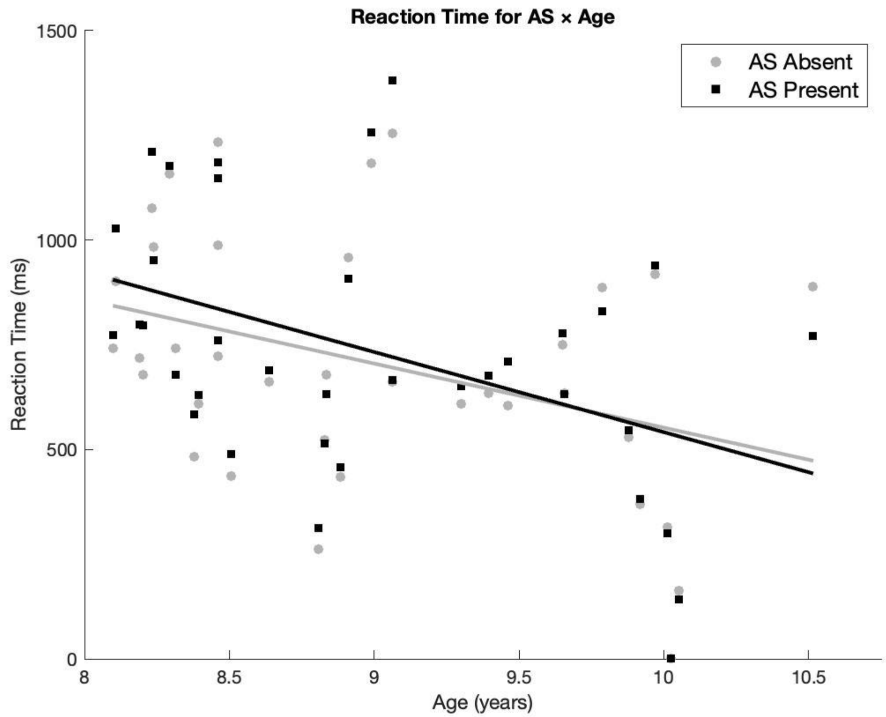

Figure 8. Age predicting RT by AS Condition. As age increases, both RT in the AS Absent and AS Present condition decrease. Younger children have differences in RT for AS Condition, but older children do not have differences between AS Condition.

assessing the within subject factors of Condition (AS Absent, AS Present) and Hb (HbO, HbR) and two covariates (RTDiff, Age). All results presented are control for the age of participants. There were 10 significant clusters all indicating moderate effect sizes. Every extracted effect was significant at a voxel-wise alpha <.05 and cluster-wise alpha < .05. Each subject's betas for condition and Hb were extracted. Post hoc pairwise comparisons and simple slopes analysis were conducted in R if necessary (v4.2.3; R Core Team 2023). For where simple slopes analysis were required to explore an interaction involving RTDiff (*M*=27.56ms, *SD*=63.45ms), the predicted estimated marginal means were extracted for HbO and HbR at RTDiff one standard deviation below the mean (RT $RTDiff_{low}$=-30ms), zero ($RTDiff_{zero}$=0ms), and one standard deviation above the mean ($RTDiff_{high}$=90ms). $RTDiff_{low}$ represents participants who were slower in the AS Absent Condition compared to the AS Present condition. $RTDiff_{zero}$ represents participants who had no differences in RT between the AS Absent and AS Present Conditions. $RTDiff_{high}$ represents participants who were slower in the AS Present Condition compared to the AS Absent Condition. Two of the 10 significant clusters displayed deactivation patterns, see **Table 2** for a breakdown of significant clusters, MNI space, and effect sizes.

Right Inferior Frontal Gyrus

There was a significant Hb effect in the right inferior frontal gyrus (*GES*=.06). Pairwise comparisons using the Bonferroni adjustment showed that there was significant activation such that HbO (*M*=0.005, *SE*=0.002) was higher than HbR (*M*=-0.003, *SE*=0.002), *p*=.002 (**Figure 9a**).

Table 2. Clusters identified in analysis of fNIRS data for the AS paradigm

Brain Region	**Effect**	**MNI Coordinates (x,y,z)**	**Volume**	***GES***	**df**	**Finding**
Right Inferior Frontal Gyrus	Hb	(41, 40, 32)	307	.06	1, 35	Activation
Right Inferior Frontal Gyrus	Hb*Cond	(48, 40, 19)	38	.05	1, 31	Activation during AS Absent
Right Inferior Frontal Gyrus	Hb*RTDiff	(50, 28, 29)	62	.07	1, 35	Activation for $RTDiff_{low}$ and $RTDiff_{zero}$
Left Inferior Frontal Gyrus	Hb*Cond*RTDiff	(-39, 38, 30)	38	.06	1, 35	Increase in HbO for AS Present for $RTDiff_{low}$ and $RTDiff_{zero}$
Left Inferior Parietal Lobe	Hb	(-37, -70, 52)	56	.06	1, 29	Deactivation
Left Inferior Parietal Lobe	Hb*RTDiff	(-47, -41, 65)	26	.06	1, 29	Deactivation
Left Angular Gyrus	Hb	(-51, -59, 47)	25	.04	1, 29	Activation
Right Angular Gyrus	Hb*RTDiff	(50, -54, 52)	143	.08	1, 35	Activation for $RTDiff_{low}$ and $RTDiff_{zero}$
Left Precuneus	Hb*RTDiff	(-24, -64, 65)	27	.04	1, 32	Activation for $RTDiff_{high}$
Right Superior Parietal Lobe	Hb*Cond*RTDiff	(32, -52, 67)	178	.07	1, 33	No significant activation pattern

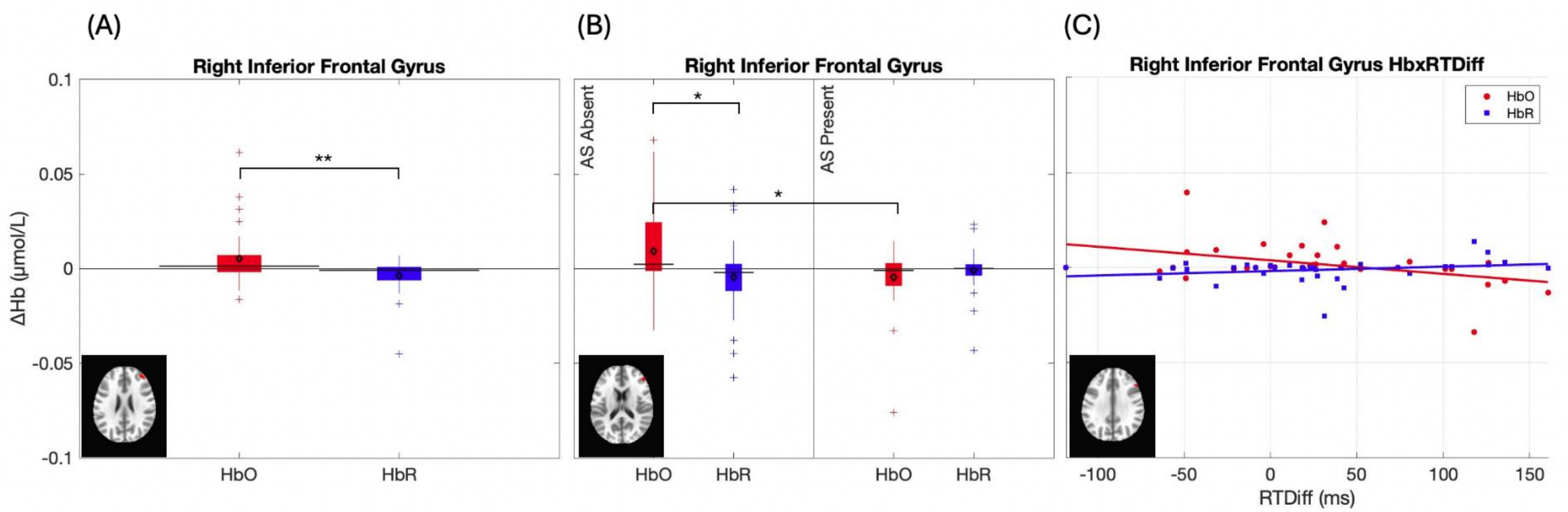

Figure 9. Right inferior frontal gyrus activation patterns during the AS paradigm. (A) Hb effect during the AS Paradigm showing activation in the right inferior frontal gyrus. (B) Hb*Condition effect showing activation during the AS Absent Condition in the right inferior frontal gyrus. (C) Hb*RTDiff effect during the AS Paradigm showing activation for $RTDiff_{low}$ (M=-30ms), and $RTDiff_{zero}$ (M=0ms) in the right inferior frontal gyrus.

There was a significant interaction between Hb and Condition (AS Absent, AS Present) effect in the right Inferior Frontal Gyrus (*GES*=.06). Pairwise comparisons revealed that there was significant activation during the AS Absent Condition such that HbO (*M*=0.009, *SE*=0.003) was higher than HbR (*M*=-0.004, *SE*=0.003), *p*=.011. In the AS Absent Condition, HbO was higher (*M*=0.009, *SE*=0.003) compared to the AS Present Condition (*M*=-0.004, *SE*=0.003), *p*=.013 (**Figure 9b**).

There was a significant interaction between Hb and RTDiff in the right inferior frontal gyrus (*GES*=.07) such that HbO levels decreased the more participants were distracted by the color singleton distractor, *p*=.0001. However, the slope for RTDiff predicting HbR was not different from zero, *p*=0.18. Contrasts revealed that RTDiff more strongly predicts HbO compared to HbR, *p*=.0002 (**Table A1**). Additional simple slopes analysis was used to assess the estimated marginal means for HbO and HbR for $RTDiff_{low}$, $RTDiff_{zero}$, and $RTDiff_{high}$ (**Table A2.1, Table A2.2**). It was found that there was significant activation for $RTDiff_{low}$ such that HbO was significantly higher than HbR, *p*=.001. In addition, it was found that there was significant activation for RTDiff such that HbO was significantly higher than HbR, *p*=.0009. However, there were no significant differences for $RTDiff_{high}$, *p*=0.19 (**Figure 9c**).

Left Inferior Frontal Gyrus

There was a significant interaction between Hb, RTDiff, and Condition (AS Absent, AS Present) in the left inferior frontal gyrus (*GES*=.06). Simple slopes analysis was conducted to find that HbO levels increase during the AS Absent Condition the more participants are distracted by the color singleton distractor, *p*=.046. However, the slope for RTDiff predicting HbR was marginal, *p*=0.08. Contrasts revealed that RTDiff more strongly predicts HbO compared to HbR, *p*=.04. The differences between the slopes for RTDiff predicting HbO during the AS Absent compared to HbO during the AS Present was also significant, *p*=.049 (**Table A3**).

Additional simple slopes analysis assessed the estimated marginal means for HbO and HbR for $RTDiff_{low}$, $RTDiff_{zero}$, and $RTDiff_{high}$ (**Table A4, Table A5**). It was found that for $RTDiff_{low}$, HbO was higher for the AS Present Condition compared to the AS Absent Condition, *p*=.009. The same pattern was found for $RTDiff_{zero}$, such that HbO was higher for the AS Present Condition compared to the AS Absent Condition, *p*=.027 (**Figure 10**).

Left Inferior Parietal Lobe

There was a significant Hb effect in the left inferior parietal lobe (*GES*=.06). However, pairwise comparisons using the Bonferroni adjustment showed that there was significant deactivation such that HbR (*M*=0.002, *SE*=0.002) was higher than HbO (*M*=-0.007, *SE*=0.002), *p*=.0004 (**Figure 11a**).

There was a significant interaction between Hb and RTDiff in the left inferior parietal lobe (*GES*=.06). Simple slopes analysis was conducted to find that RTDiff predicts HbO during the AS Absent Condition such that HbO levels increase the more participants are distracted by the color singleton distractor, *p*=.0006. However, the slope for RTDiff predicting HbR was not different from zero, *p*=0.73. Contrasts revealed that

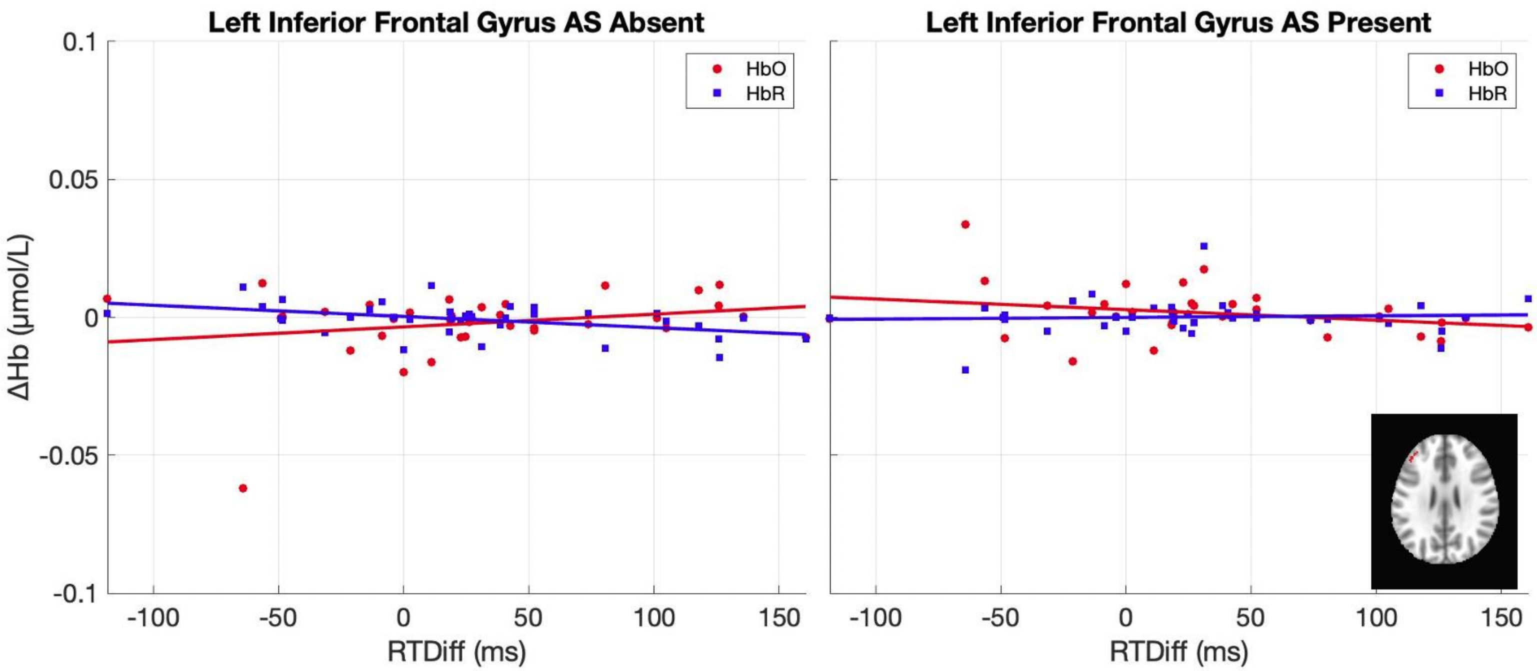

Figure 10. Left inferior frontal gyrus activation patterns during the AS paradigm. Hb*Condition*RTDiff effect during the AS Paradigm in the left inferior frontal gyrus such that for $RTDiff_{low}$ (M=-30ms), and $RTDiff_{zero}$ (M=0ms), HbO was higher for the AS Present Condition compared to the AS Absent Condition.

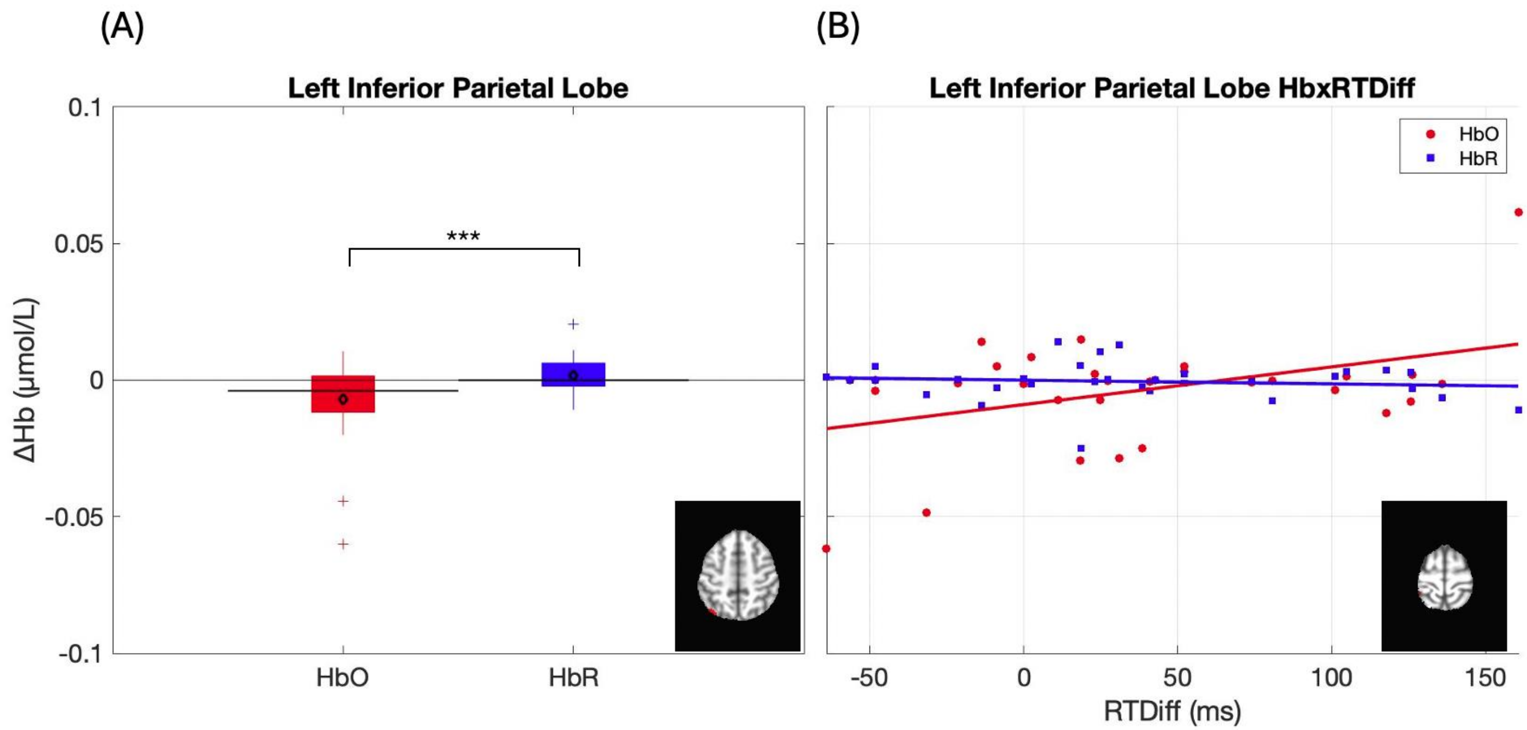

Figure 11. Left inferior parietal lobe activation patterns during the AS paradigm. (A) Hb effect showing deactivation in the left inferior parietal lobe during the AS Paradigm. (B) Hb*RTDiff effect during the AS Paradigm in the left inferior parietal lobe showing deactivation for $\text{RTDiff}_{\text{low}}$ (M=-30ms), and $\text{RTDiff}_{\text{zero}}$ (M=0ms).

RTDiff more strongly predicts HbO compared to HbR, p=.007 (**Table A6**). Further simple slope analysis revealed deactivation patterns for both $\text{RTDiff}_{\text{low}}$, and $\text{RTDiff}_{\text{zero}}$, p=0.007; p=0.023 respectively (**Table A7.1, Table A7.2**). However, there were no significant differences for Hb for $\text{RTDiff}_{\text{high}}$, p=0.30 (**Figure 11b**).

Left Angular Gyrus

There was a significant Hb effect in the left angular gyrus (*GES*=.04). Pairwise comparisons using the Bonferroni adjustment showed that there was significant activation such that HbO (*M*=0.006, *SE*=0.003) was higher than HbR (*M*=-0.002, *SE*=0.003), p=.012 (**Figure 12**).

Right Angular Gyrus

There was a significant interaction between Hb and RTDiff in the right angular gyrus (*GES*=.08). Simple slopes analysis was conducted to find that RTDiff predicts HbO such that HbO levels decrease the more participants are distracted by the color singleton distractor, p=.012. However, the slope for RTDiff predicting HbR was not different from zero, p=0.63. Contrasts revealed that RTDiff more strongly predicts HbO compared to HbR, p=.034 (**Table A8**). Additional simple slopes analysis assessed the estimated marginal means for HbO and HbR for $\text{RTDiff}_{\text{low}}$, $\text{RTDiff}_{\text{zero}}$, and $\text{RTDiff}_{\text{high}}$ (**Table A9.1, Table A9.2**). It was found that there was significant activation for $\text{RTDiff}_{\text{low}}$ such that HbO was significantly higher than HbR, p=.006. In addition, it was found that there was significant activation for $\text{RTDiff}_{\text{zero}}$ such that HbO was significantly higher than HbR, p=.013. However, there were no differences for Hb for $\text{RTDiff}_{\text{high}}$, p=0.81 (**Figure 13**).

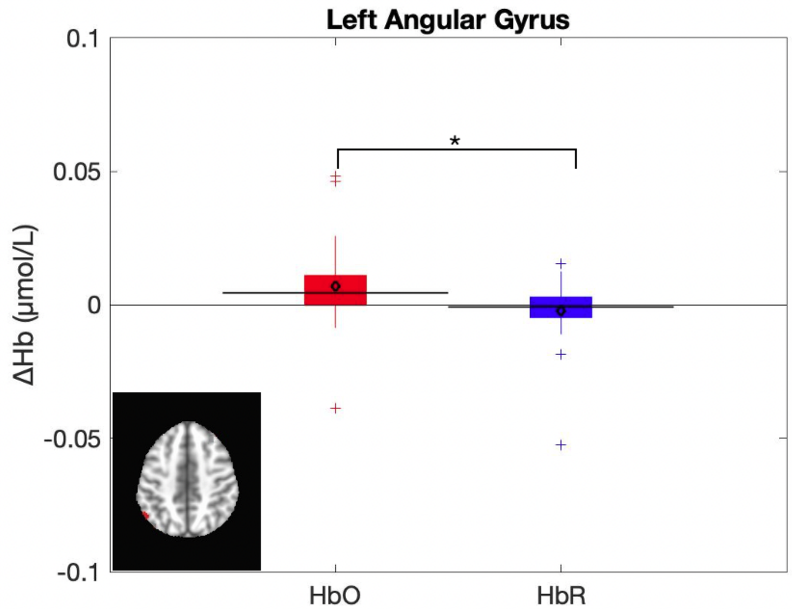

Figure 12. Left angular gyrus activation pattern during the AS paradigm. Hb effect showing activation in the left angular gyrus during the AS Paradigm.

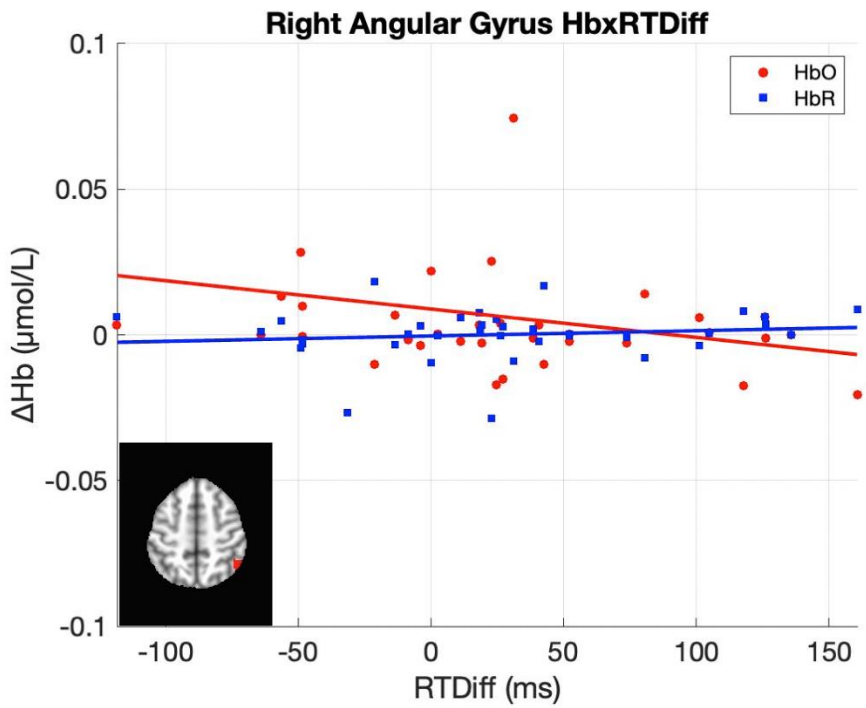

Figure 13. Right angular gyrus activation pattern during the AS paradigm. Hb*RTDiff effect during the AS Paradigm in the right angular gyrus showing activation for $RTDiff_{low}$ (M=-30ms), and $RTDiff_{zero}$ (M=0ms).

Left Precuneus

There was a significant interaction between Hb, and RTDiff in the left precuneus (*GES*=.04). Simple slopes analysis was conducted to find that RTDiff predicts HbO such that HbO levels increase the more participants are distracted by the color singleton distractor, p=.005. However, the slope for RTDiff predicting HbR was not different from zero, p=0.34. Contrasts revealed that RTDiff more strongly predicts HbO compared to HbR, p=.008 (**Table A10**). Additional simple slopes analysis assessed the estimated marginal means for HbO and HbR for $RTDiff_{low}$, $RTDiff_{zero}$, and $RTDiff_{high}$ (**Table A11.1, Table A11.2**). It was found that there was significant activation for $RTDiff_{high}$ such that HbO was significantly higher than HbR, p=.006. However, there were no differences in Hb for $RTDiff_{low}$, or $RTDiff_{zero}$, p=0.12; p=0.41 respectively (**Figure 14**).

Right Superior Parietal Lobe

There was a significant interaction between Hb, RTDiff, and Condition (AS Absent, AS Present) in the right superior parietal lobe (*GES*=.07). Simple slopes analysis was conducted to find that RTDiff predicts HbO during the AS Present Condition such that HbO levels increase the more participants are distracted by the color singleton distractor, p=.014 (**Table A12**).

Additional simple slopes analysis assessed the estimated marginal means for HbO and HbR for $RTDiff_{low}$, $RTDiff_{zero}$, and $RTDiff_{high}$ (**Table A13, Table A14**). However, there were no significant activation patterns seen across the different levels of RTDiff. Visually, there seems to be an activation pattern present for $RTDiff_{low}$ during the AS

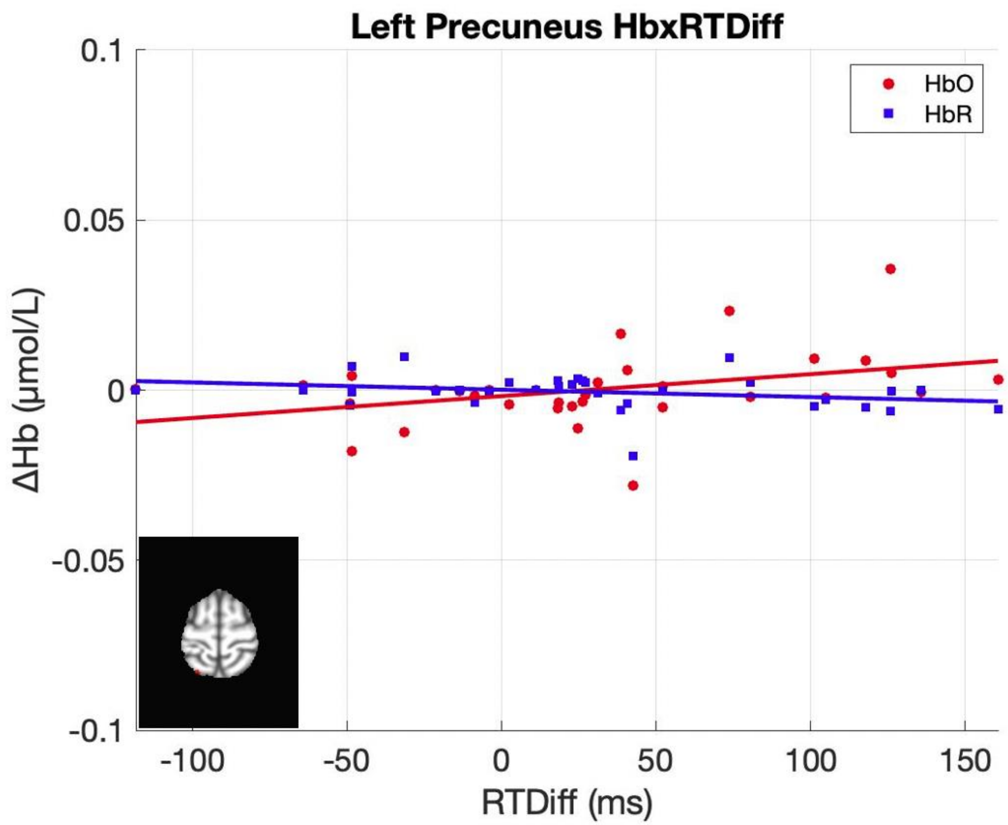

Figure 14. Left precuneus activation pattern during the AS paradigm. Hb*RTDiff effect during the AS Paradigm in the left precuneus showing activation for RTDiffhigh (M=90ms).

Absent Condition, p=0.48. In addition, there seems to be an activation pattern present for $RTDiff_{high}$ during the AS Present Condition, p=0.18 (**Figure 15**).

Exploring the Brain-Behavior Relationship of the Dimensional Label Understanding tasks

To explore the neural differences between the DLU tasks (Color Production, Color Comprehension, Shape Production, Shape Comprehension) and whether those differences can be predicted by distractibility (RTDiff), a 3dMVM (a mixed effects ANOVA) in AFNI (Chen et al., 2014) was conducted with Hb as a within-subject factor with two levels (HbO, HbR), and two covariates (RTDiff, Age). All results presented control for age of the participant. There were 9 significant clusters all with moderate effect sizes. Every extracted effect was significant at a voxel-wise alpha <.05 and cluster-wise alpha < .05. There were 10 significant clusters all indicating moderate effect sizes. Every extracted effect was significant at a voxel-wise alpha <.05 and cluster-wise alpha < .05. Each subject's betas for condition and Hb were extracted. Post hoc pairwise comparisons and simple slopes analysis were conducted in R if necessary (v4.2.3; R Core Team 2023). For where simple slopes analysis were required to explore an interaction involving RTDiff (M=27.56ms, SD=63.45ms), the predicted estimated marginal means were extracted for HbO and HbR at RTDiff one standard deviation below the mean (RT $RTDiff_{low}$=-30ms), zero ($RTDiff_{zero}$=0ms), and one standard deviation above the mean ($RTDiff_{high}$=90ms). $RTDiff_{low}$ represents participants who were slower in the AS Absent

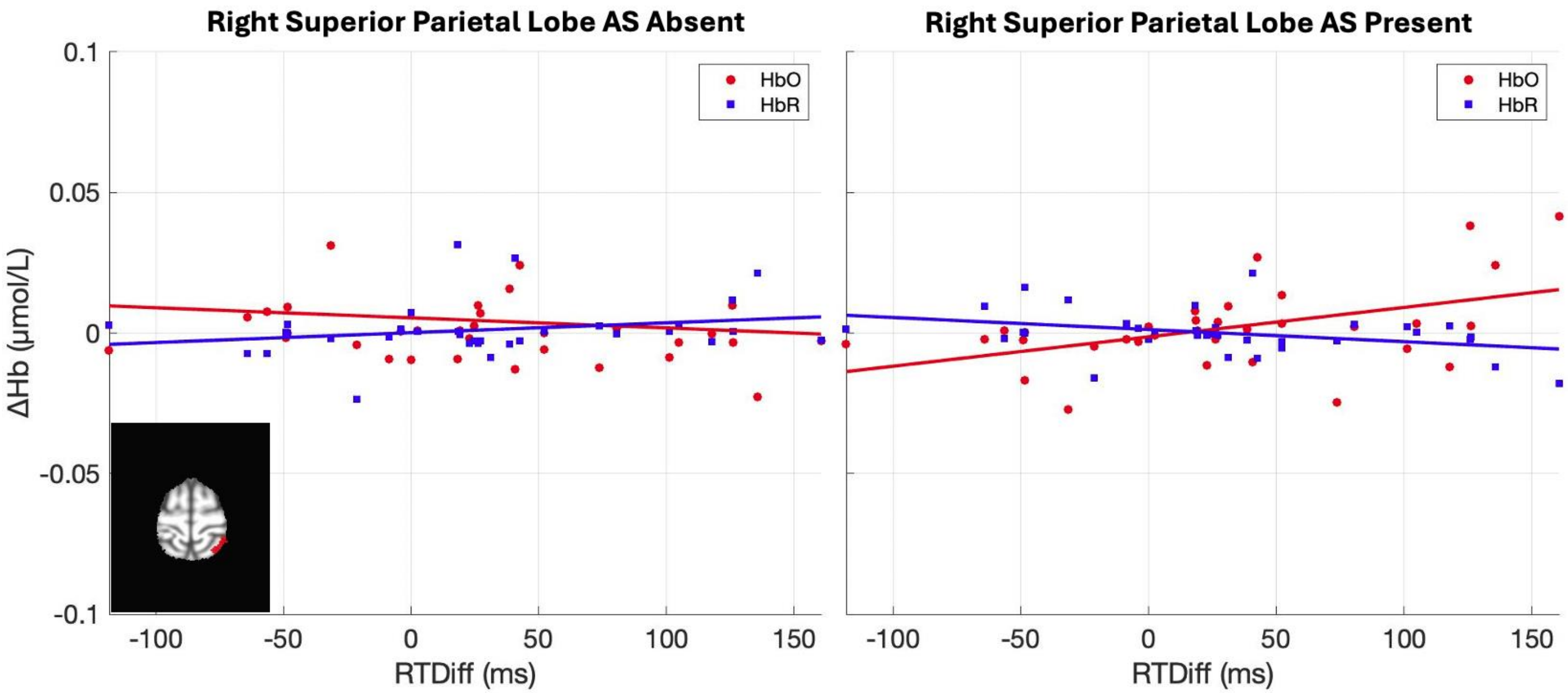

Figure 14. Right superior parietal lobe activation patterns during the AS paradigm. Hb*Condition*RTDiff effect during the AS Paradigm in the right superior parietal lobe. No pairwise comparisons were significant but there seems to be a general activation pattern for $RTDiff_{low}$ (M=-30ms) during the AS Absent Condition and $RTDiff_{high}$ (M=90ms) during the AS Present Condition.

Condition compared to the AS Present condition. $RTDiff_{zero}$ represents participants who had no differences in RT between the AS Absent and AS Present Conditions. $RTDiff_{high}$ represents participants who were slower in the AS Present Condition compared to the AS Absent Condition. Three of the 9 significant clusters displayed deactivation patterns, see **Table 3** for a breakdown of significant clusters, MNI space, and effect sizes.

Right Angular Gyrus

There was a main effect of Hb in the right angular gyrus (*GES*=.11). Pairwise comparisons using the Bonferroni adjustment found activation in this region such that HbO (M=0.018, SE=0.003) was significantly larger than HbR (M=-0.009, SE=0.003), p<.0001 (**Figure 16**).

Right Anterior Superior Parietal Lobe

There was a significant interaction between Hb, and RTDiff in the right anterior superior parietal lobe (*GES*=.11). Simple slopes analysis was conducted to show that RTDiff significantly predicts HbO such that HbO levels decrease the more participants are distracted by the color singleton distractor, p<.0001. However, the slope for HbR was not different from zero, p=.17. In addition, contrasts revealed that the slopes for RTDiff predicting HbO and HbR were different from each other, p<.0001 (**Table A15**). An additional simple slopes analysis assessed the estimated marginal means for HbO and HbR for $RTDiff_{low}$, $RTDiff_{zero}$, and $RTDiff_{high}$ (**Table A16.1, TableA16.2**). It was found that there was activation for both $RTDiff_{low}$, and $RTDiff_{zero}$ such that HbO was

Table 3. Clusters identified in analysis of fNIRS data for the Dimensional Label Understanding Tasks

Brain Region	**Effect**	**MNI Coordinates (x,y,z)**	**Volume**	***GES***	***df***	**Finding**
Right Angular Gyrus	Hb	(47, -50, 57)	385	.11	1, 35	Activation
Right Anterior Superior Parietal Lobe	Hb*RTDiff	(33, -41, 69)	180	.11	1, 27	Activation for $RTDiff_{low}$ and $RTDiff_{zero}$
Right Posterior Superior Parietal Lobe	Hb*RTDiff	(31, -59, 63)	40	.08	1, 35	Activation for $RTDiff_{high}$
Right Postcentral Gyrus	Hb*RTDiff	(3, -56, 73)	81	.09	1, 15	Activation for $RTDiff_{high}$
Left Middle Frontal Gyrus	Hb	(-21, 49, 36)	137	.11	1, 29	Deactivation
Left Middle Frontal Gyrus	Hb*RTDiff	(-23, 41, 43)	86	.09	1, 33	Deactivation
Right Middle Frontal Gyrus	Hb*RTDiff	(38, 36, 42)	100	.09	1, 35	Activation for $RTDiff_{low}$ and $RTDiff_{zero}$
Left Precentral Gyrus	Hb	(-45, 18, 44)	51	.11	1, 26	Deactivation
Left Inferior Frontal Gyrus	Hb*RTDiff	(-44, 31, 30)	82	.10	1, 35	Activation for $RTDiff_{low}$

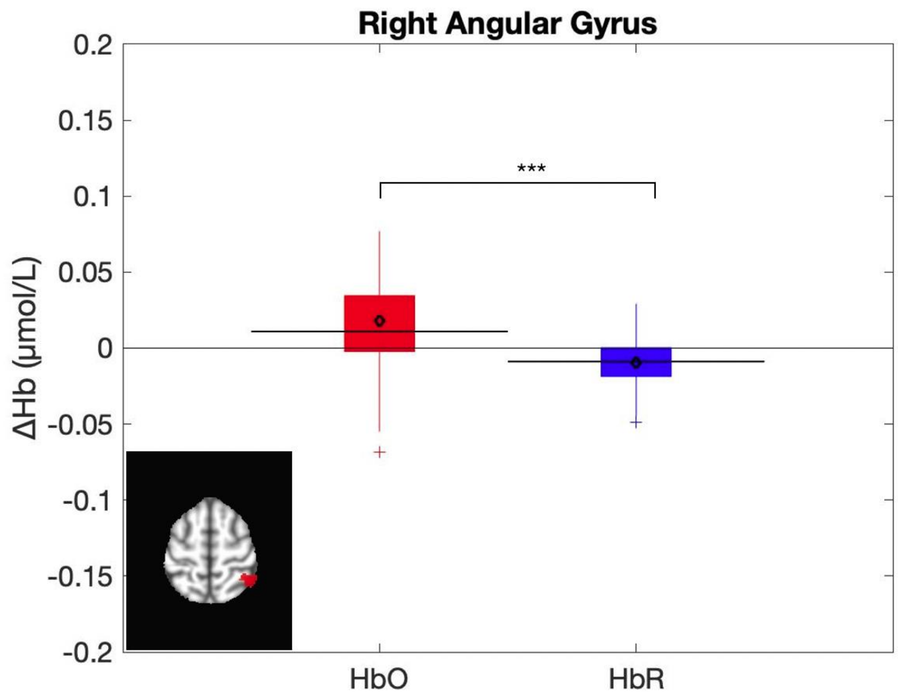

Figure 15. Right angular gyrus activation pattern during the DLU task. Hb effect found activation in the right angular gyrus.

higher than HbR, $p<.0001$; $p=.0096$ respectively. On the other hand, there was significant deactivation for $RTDiff_{high}$ such that HbR was higher than HbO, $p<.0001$ (**Figure 17a**).

Right Posterior Superior Parietal Lobe

There was a significant interaction between Hb, and RTDiff in the right posterior superior parietal lobe (*GES*=.08). Simple slopes analysis was conducted found that RTDiff significantly predicts HbO such that HbO levels increase the more participants are distracted by the color singleton distractor, $p=.0003$. However, the slope for HbR was not different from zero, $p=.13$. In addition, contrasts revealed that the slopes for RTDiff predicting HbO and HbR were different from each other, $p=.0003$ (**Table A17**). Additional simple slopes analysis assessed the estimated marginal means for HbO and HbR for $RTDiff_{low}$, $RTDiff_{zero}$, and $RTDiff_{high}$ (**Table A18.1, Table A18.2**). It was found that there was significant activation for $RTDiff_{high}$ such that HbO was higher than HbR, p=.0011(**Figure 17b**).

Right Postcentral Gyrus

There was a significant interaction between Hb, and RTDiff in the right postcentral gyrus (*GES*=.09). Simple slopes analysis was conducted to show that RTDiff significantly predicts HbO such that HbO levels increase the more participants are distracted by the color singleton distractor, $p<.0001$. However, the slope for HbR was not different from zero, $p=.40$. In addition, contrasts revealed that the slopes for RTDiff predicting HbO and HbR were different from each other, $p<.0001$ (**Table A19**). Additional simple slopes analysis assessed the estimated marginal means for HbO and

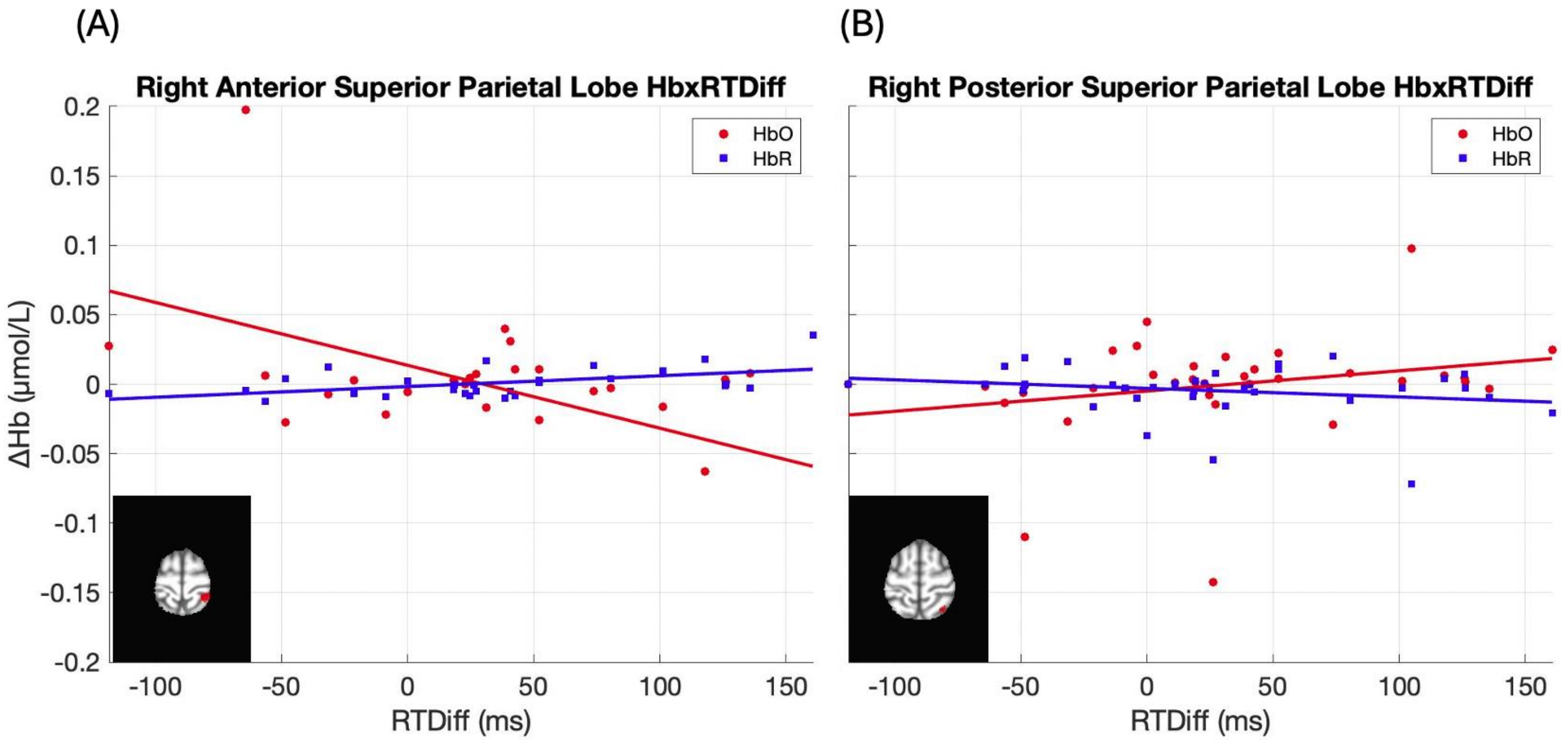

Figure 16. Superior parietal lobe activation patterns during the DLU task. (A) Hb*RTDiff effect found in the right superior parietal lobe during the Dimensional Label Understanding task showing activation for $RTDiff_{low}$ (M=-30ms) and $RTDiff_{zero}$ (M=0ms). (B) Hb*RTDiff effect found in the right superior parietal lobe during the Dimensional Label Understanding task showing activation for $RTDiff_{high}$ (M=90ms).

HbR for $RTDiff_{low}$, $RTDiff_{zero}$, and $RTDiff_{high}$ (**Table A20.1, Table A20.2**). It was found that there was significant deactivation for $RTDiff_{low}$ such that HbR was higher than HbO, p=.0095. Conversely, there was significant activation for $RTDiff_{high}$ such that HbO was higher than HbR, p<.0001(**Figure 18**).

Left Middle Frontal Gyrus

There was a main effect of Hb in the left middle frontal gyrus (*GES*=.11). Pairwise comparisons using the Bonferroni adjustment found deactivation in this region such that HbR (*M*=0.010, *SE*=0.002) was higher than HbO (*M*=-0.009, *SE*=0.002), p<.0001(**Figure 19a**).

There was a significant interaction between Hb, and RTDiff in the left middle frontal gyrus (*GES*=.09). Simple slopes analysis was conducted to find that RTDiff significantly predicts HbO such that HbO levels decrease the more participants are distracted by the color singleton distractor, p<.0001. However, the slope for HbR was not different from zero, p=.44. In addition, contrasts revealed that the slopes for RTDiff predicting HbO and HbR were different from each other, p<.0001(**Table A21**). Additional simple slopes analysis analyzed the estimated marginal means for HbO and HbR for $RTDiff_{low}$, $RTDiff_{zero}$, and $RTDiff_{high}$ (**Table A22.1, Table A22.2**). There were significant deactivation patterns for both $RTDiff_{zero}$, and $RTDiff_{high}$ such that HbR was higher than HbO, p=.01; p<.0001, respectively (**Figure 19b**).

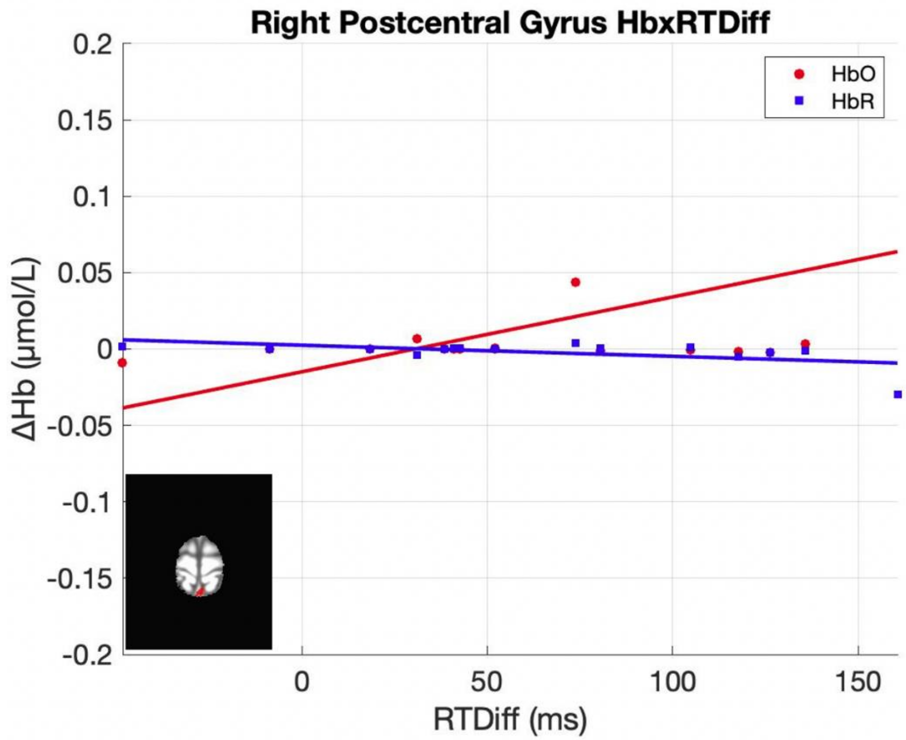

Figure 17. Right postcentral gyrus activation pattern during the DLU task. Hb*RTDiff effect found in the right postcentral gyrus showing activation for $RTDiff_{high}$ (M=90ms).

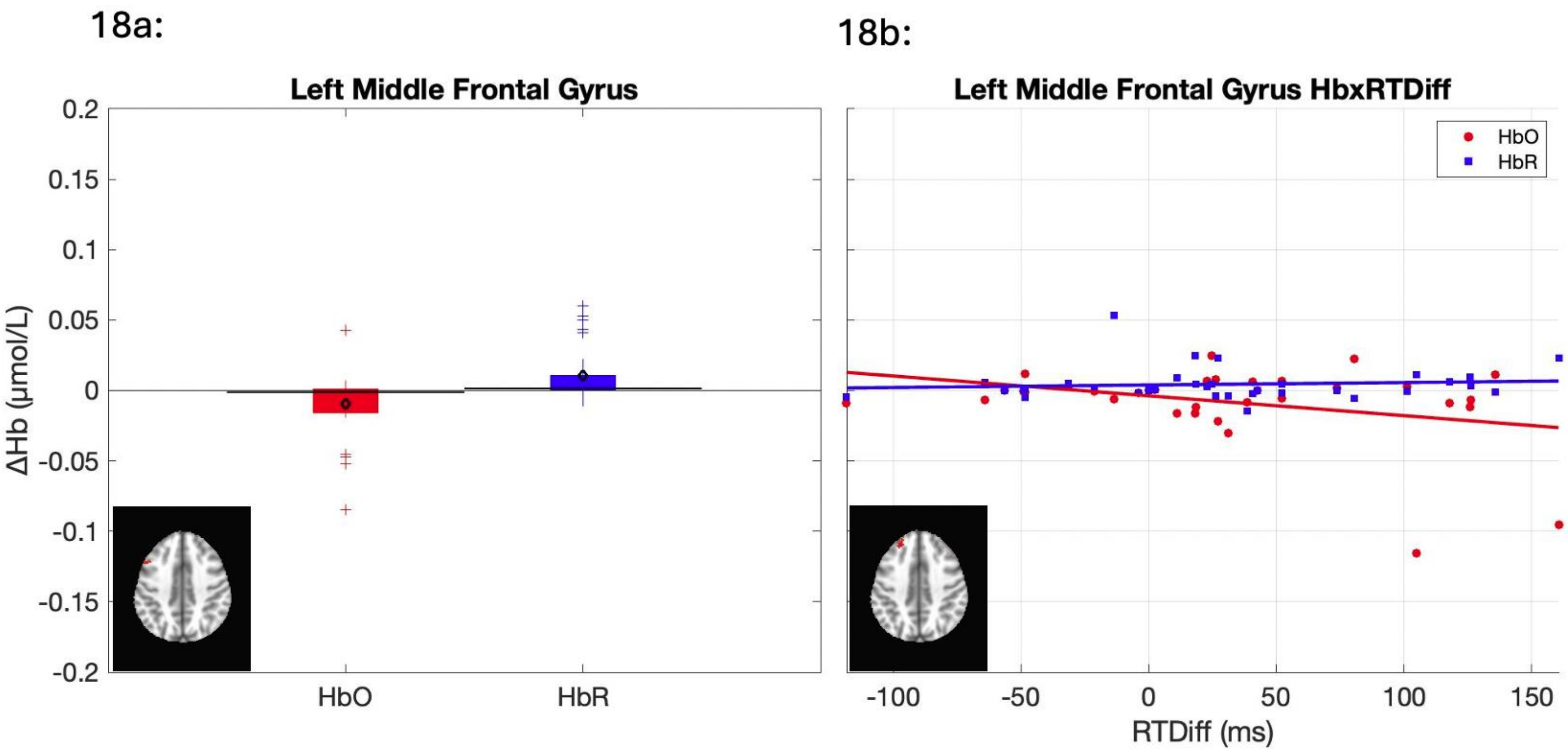

Figure 18. Left middle frontal gyrus activation patterns during the DLU task. (A) Hb effect in the left middle frontal gyrus found deactivation during the Dimensional Label Understanding tasks. (B) Hb*RTDiff effect found in the left middle frontal gyrus during the Dimensional Label Understanding task showing deactivation for $RTDiff_{zero}$ (M=0ms), and $RTDiff_{high}$ (M=90ms).

Right Middle Frontal Gyrus

There was a significant interaction between Hb, and RTDiff in the right middle frontal gyrus (*GES*=.09). Simple slopes analysis was conducted and found that RTDiff significantly predicts HbO such that HbO levels decrease the more participants are distracted by the color singleton distractor, p<.0001. However, the slope for HbR was not different from zero, p=.17. In addition, contrasts revealed that the slopes for RTDiff predicting HbO and HbR were different from each other, p<.0001 (**Table A23**). Additional simple slopes analysis assessed the estimated marginal means for HbO and HbR for $RTDiff_{low}$, $RTDiff_{zero}$, and $RTDiff_{high}$ (**Table A24.1, Table A24.2**). It was found that there was activation for both $RTDiff_{low}$ and $RTDiff_{zero}$ such that HbO was higher than HbR, p<.0001; p=.0023 respectively. On the other hand, there was significant deactivation for $RTDiff_{high}$ such that HbR was higher than HbO, p<.0001(**Figure 20**).

Left Precentral Gyrus

There was a main effect of Hb in the left precentral gyrus (*GES*=.11). Pairwise comparisons using the Bonferroni adjustment found deactivation in this region such that HbR (*M*=0.011, *SE*=0.004) was higher than HbO (*M*=-0.025, *SE*=0.004), p<.0001.

Left Inferior Frontal Gyrus

There was a significant interaction between Hb, and RTDiff in the left inferior frontal gyrus (*GES*=.10). Simple slopes analysis was conducted and found that RTDiff significantly predicts HbO such that HbO levels decrease the more participants are distracted by the color singleton distractor, p<.0001. However, the slope for HbR was not

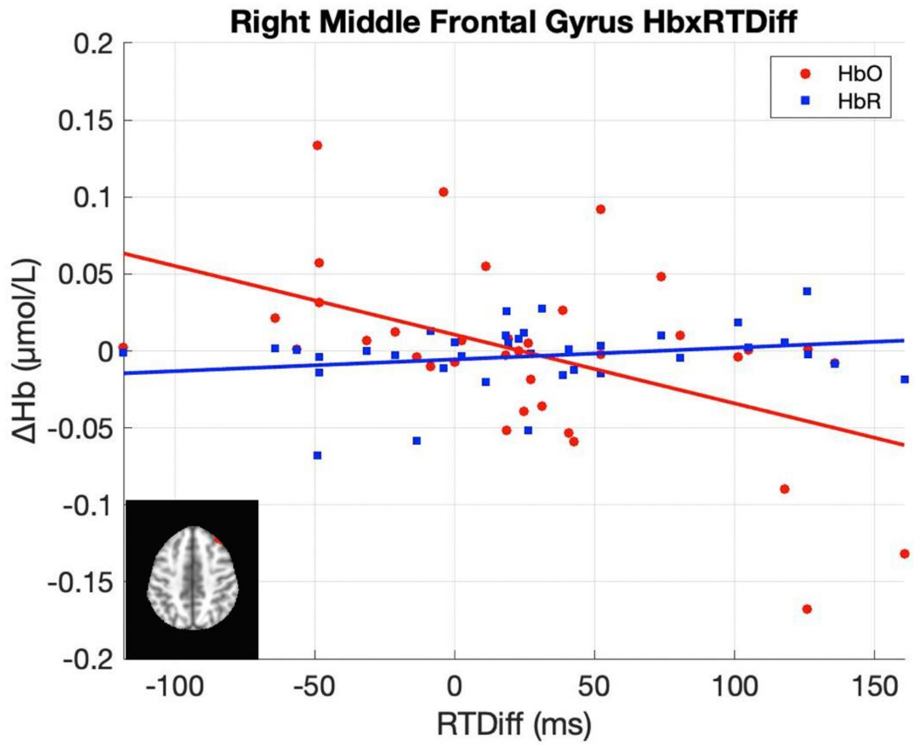

Figure 19. Right middle frontal gyrus activation pattern during the DLU task. Hb*RTDiff effect found in the right middle frontal gyrus during the Dimensional Label Understanding task showing activation for $RTDiff_{low}$ (M=-30ms), and $RTDiff_{zero}$ (M=0ms).

different from zero, p=.87. In addition, contrasts revealed that the slopes for RTDiff predicting HbO and HbR were different from each other, p<.0001 (**Table A25**). Additional simple slopes analysis assessed the estimated marginal means for HbO and HbR for $RTDiff_{low}$, $RTDiff_{zero}$, and $RTDiff_{high}$ (**Table A26.1, Table A26.2**). It was found that there was activation for $RTDiff_{low}$ such that HbO was higher than HbR, p=.0028. On the other hand, there was significant deactivation for $RTDiff_{high}$ such that HbR was higher than, p<.0001 (**Figure 21**).

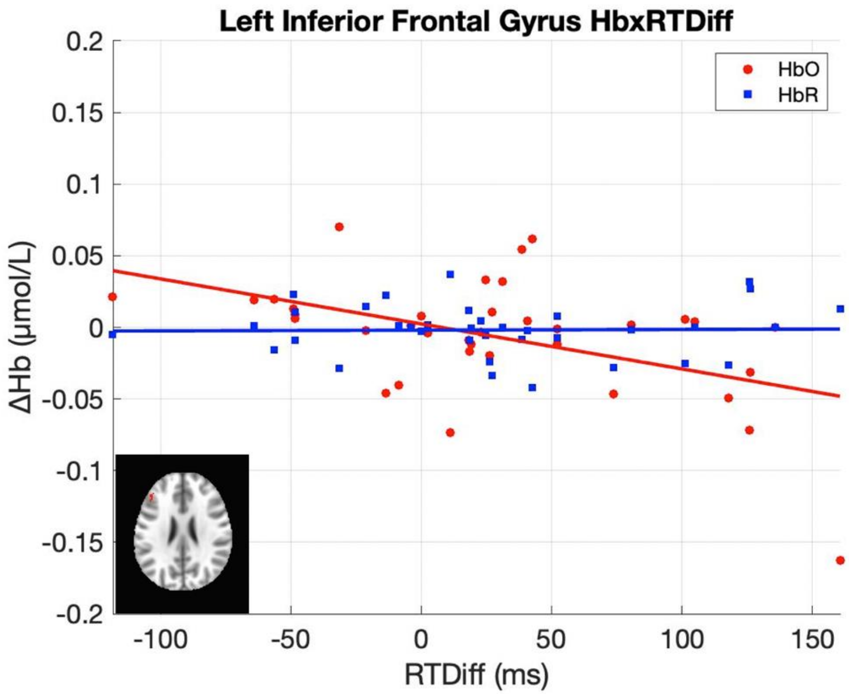

Figure 20. Left inferior frontal gyrus activation pattern during the DLU task. Hb*RTDiff effect found in the left inferior frontal gyrus during the Dimensional Label Understanding task showing activation for $RTDiff_{low}$ (M=-30ms), and $RTDiff_{zero}$ (M=0ms

CHAPTER FOUR:

DISCUSSION

Previous work has focused on analyzing the impact of label understanding on selectively attending towards relevant information in the environment while the current study instead explored the impact of label understanding on the ability to inhibit irrelevant information in the environment.

Behavioral Results Summary

The behavioral results found in the AS paradigm were successfully replicated indicating that participants were overall slower during the AS Present Condition compared to the AS Absent condition. However, there were no detectable differences in accuracy between the AS Absent and AS Present conditions due to the overall high accuracy and low variability of performance in participants. In addition, the current study found that the AS Present Condition was more distracting for the younger children compared to the older children. These results underline the developmental shift occurring between 8- to 10- years old in the ability to inhibit distractors.

Neural Results of the Additional Singleton Paradigm Summary

The second aim of the study was to assess the neural mechanisms of attentional selection and inhibitory control in children, by exploring whether individual differences in how children respond to a salient distractor yields different neural results during the AS paradigm. Children with low distractibility in the AS Present task may be displaying a learned suppression technique, such that participants actively suppress the color singleton distractor (Gaspelin & Luck, 2018; Stilwell et al., 2022).

Frontal Cortex Activation

There were significant activation patterns seen in both the right and left inferior frontal gyrus. In the left inferior frontal gyrus, there was higher HbO seen during the AS Present Condition compared to the AS Absent Condition for children with low distractibility (RTDiff) for the color singleton distractor. These results are in line with the findings of Lavie & de Fockert (2006) who demonstrated a negative correlation between activation in the left frontal cortex and distractibility of the color singleton. Therefore, it seems that children who are less distracted by the color singleton distractor are displaying more adult-like neural activation patterns in the frontal cortex.

There was overall activation in the right inferior frontal gyrus during the AS Absent Condition, and for participants with low distractibility during the AS paradigm. However, there was not a significant three-way interaction to assess the relationship between Condition x Distractibility (RTDiff) x Hb. Despite this, it seems that the children with low distractibility towards the color singleton distractor are also activating the right inferior frontal gyrus. The inferior frontal cortex is required for selectively attending towards targets and is part of the system involved in detecting behaviorally relevant stimuli (Corbetta & Shulman, 2003; Zhang et al., 2004). Therefore, children who were less distracted by the color singleton distractor seem to be utilizing a more bottom-up attentional process. Similarly, the importance of the frontal cortex in bottom-up attention suggests that children are utilizing this attentional strategy to suppress the salient distractor, or more easily select the target.

Parietal Lobe Activation

Additional activation patterns were present in the left and right angular gyrus. Specifically, children with low distractibility towards the color singleton showed activation in the right angular gyrus across conditions. The angular gyrus is in the posterior part of the inferior parietal lobe and is situated to receive input from surrounding regions to integrate multimodal information (Rockland & Graves, 2023). The right angular gyrus has been of interest in visuospatial attention research which suggests that the right angular gyrus is crucial for disengagement and reorienting of attention (Wagner & Rusconi, 2023). Taken together with the results of the current study, this indicates that children with lower distractibility towards the color singleton distractor are successfully reorienting attention to find the target.

Exploring further activation in the parietal lobe, there was an activation pattern in the left precuneus for children who were highly distracted by the color singleton distractor. In addition to this, a three-way interaction found in the right superior parietal lobe followed a similar pattern such that higher distractibility was associated with higher HbO. The precuneus is a region located medially in the parietal cortex situated between the sensorimotor region and parieto-occipital cortex (Dadario & Sughrue, 2023). The coordinates of activation in the current study for the left precuneus were less medial and adjacent to the left superior parietal lobe. Functional imaging studies have observed activation in the precuneus and the superior parietal lobe during the execution or preparation of spatially guided behaviors (Cavanna & Trimble, 2006). Research by de Fockert et al. (2004) found that the superior parietal lobe was associated with shifts of attention and activated during the irrelevant color singleton distractor condition during the AS paradigm. Given that the location of the activation for children who had high distractibility towards the color singleton distractor is bordering on the superior parietal lobe and precuneus region, it is possible that we are seeing activation in these regions due to the children's attention being allocated towards the color singleton.

Neural Results of the Dimensional Label Understanding Tasks Summary

The neural results during the AS paradigm provide a base from which to further explore the relationship between distractibility in the AS paradigm and label understanding in the DLU tasks. Therefore, the third aim of the current study assessed the neural activation during the DLU tasks and if activation can be predicted by distractibility towards the color singleton in the AS paradigm. These results represent an exploratory analysis, in which we expect individual differences in brain activity despite all participants reaching ceiling behaviorally. This is because as children develop their label representations, it is likely that they develop different neural patterns due to the differences in experience and circumstances around how they learned their label representations.

Frontal Cortex Activation

In the right middle frontal gyrus and left inferior frontal gyrus, there was activation during the DLU tasks for participants who were not distracted by the color singleton distractor in the AS paradigm. McCraw et al. (2023) found that left inferior frontal cortex activity during the Dimensional Label Production task predicted higher performance in the DCCS while Lowery et al. (2022) found that activation in the left middle frontal gyrus during the Dimensional Label Production task predicted higher performance in the DCCS. The current study found right middle gyrus activation, but this still suggests a similar pattern such that participants who were not distracted by the irrelevant color singleton in the AS paradigm also activated the left inferior frontal gyrus and middle frontal gyrus during the DLU tasks. These findings replicate the link between frontal cortex activation and dimensional attention performance, as a similar pattern was found with performance in a visual search task. Therefore, this suggests that children with low distractibility are displaying similar activation patterns as children who perform well in other dimensional attention tasks.

Parietal Lobe Activation

It was found that there was general activation across participants in the right angular gyrus. As previously discussed, the angular gyrus is situated to receive information from surrounding regions and has a wide range of functions (Rockland & Graves, 2023). There is a relationship between activation in the angular gyrus and word recognition and semantic retrieval (Desai et al., 2023; Rockland & Graves, 2023).

Therefore, it seems that the participants in the current study could be activating the angular gyrus to recall color and shape labels.

In addition, there was an activation pattern present in the right superior parietal lobe during the DLU tasks. Participants with low distractibility towards the color singleton activated the more anterior/rostral part of the right superior parietal lobe. Interestingly, the participants with high distractibility towards the color singleton had activation in the posterior part of the right superior parietal lobe next to the intraparietal sulcus as well as activation in the postcentral gyrus bordering the superior parietal lobe. Based on these results, we have two different and conflicting activation patterns in similar areas of the brain. Due to potential error in how activation is mapped onto the Colins atlas, it must be determined that all participants activated the superior parietal lobe area during the DL task in the current study. Attention towards a stimulus has been associated with the superior parietal lobe, with activation extending towards the postcentral gyrus (Corbetta & Shulman, 2002). Therefore, in the DLU tasks, it could be that all participants are using these attentional networks of top-down processing to complete the DLU tasks.

The Role of Top-Down and Bottom-Up Attention for Distractor Suppression and DLU

During the AS Paradigm, children who were not distracted by the color singleton activated bilateral inferior frontal gyrus, and bilateral angular gyrus (near the temporal lobe). Similarly, during the DLU tasks, the children who were less distracted by the irrelevant singleton distractor in the AS paradigm tend to be activating a fronto-temporal-parietal network that could indicate that these children are using spatial attentional control to perform the DLU tasks (Corbetta & Shulman, 2002; Katsuki & Constantinidis, 2013; Szczepanski et al., 2014). On the other hand, the children who were more distracted by the irrelevant singleton distractor are only activating the superior parietal lobe during the DLU tasks.

Corbetta & Shulman (2002) discuss a system involving mainly right-lateralized temporal-parietal cortex and inferior frontal cortex that is used for the detection of behaviorally relevant information in the environment. The children with low distractibility towards the color singleton distractor seem to be utilizing this right-lateralized fronto-parietal network during the DLU tasks and during the AS Paradigm. This could be due to an increase in label representations such that the behaviorally relevant information (color, shape) guides their attention in a more bottom-up fashion rather than a strict top-down attentional control, such that their dimensional label understanding causes the color and shape features to be more salient. Therefore, the target (gray circle) is easier to selectively attend to.

It is possible that this increase in salience of relevant features aids in the suppression of distractors as well. For the AS paradigm, children with low distractibility activated the inferior frontal gyrus and the angular gyrus, utilizing inhibition and reorienting of attention. If children experienced an increase in salience of the relevant feature of the target (e.g., gray circle) it could cause the inhibition of irrelevant information (e.g., red diamond) and with faster reorientation.

There seems to be an interaction between the top-down goal of finding the target, and the bottom-up salience of relevant feature information (e.g., gray circle). Top-down goals in the task can potentially influence the bottom-up salience of the target information. There is an interplay of bottom-up and top-down processes seen by the fronto-parietal network activation in both the AS paradigm and DLU task for children who are not distracted by the color singleton. Indeed, when searching for an object in the environment, having a strong representation of a relevant feature aids in increasing the saliency of that feature in the environment. For example, when looking for a red apple at the grocery store, the feature, “red” increases in salience and draws the observer’s attention. Other pop-out features may not be enough to capture attention if the observer’s representation of “red” is strong enough. In a similar way, children who have a strong representation of shape (e.g., circle) may be able to increase the salience of shape such that a pop-out color (e.g., red) will not draw attention in a way they cannot control.

Limitations and Future Directions

The current study sought to include ERP analysis of the N2pc component to better understand the neural shifts seen in this age group, however, due to experimental trial-and-error, the EEG data could not be analyzed. There is a gap in the N2pc research such that the age range of 8- to 10- years-old is poorly researched despite the N2pc ERP component developing during this age range (Couperus & Quirk, 2015; Deveney et al., 2019; M. Sun et al., 2018; Turoman et al., 2021). Future research should address this gap to better understand why this developmental shift is occurring.

Further, although the current study touched on the concept of learned suppression of the additional singleton distractor, measured by RT Difference score, the current study was not equipped to do a deep dive into the neural mechanisms of individual differences in when children learn to suppress the distractor. Future research should explore the impact of attentional strategies depending on when children learn to suppress the distractor. This research could reveal developmental shifts in the ability to suppress irrelevant information.

In addition, the current study failed to replicate the findings in Heim et al., (2023) which found that parietal lobe activity was associated with selective attention. The present study found parietal lobe activity in the DLU tasks for all participants, regardless of distractibility levels. In the current study, the differences between participants with low distractibility and high distractibility during the DLU tasks were observed in the frontal cortex. Therefore, future research should analyze the role of selective attention in the inhibition of distractors.

Lastly, the findings of this study should be replicated with a complex dimensional label task that lends itself to more behavioral variability in participants such as the continuous Color Comprehension task, which allows for participants to find colors using a color spectrum rather than a search array (Lowery, 2022) or a DLU task that measures label use for known (e.g., square) and unknown, nonsense shapes (e.g., wug) in older children. With a task such as this, neural patterns for strong and weak label representation can be quantified and used to better understand the interaction between DLU, attentional selection, and inhibitory control.

REFERENCES

Bacon, W. F., & Egeth, H. E. (1994). Overriding stimulus-driven attentional capture. *Perception & Psychophysics, 55*(5), 485–496. https://doi.org/10.3758/BF03205306

Blakley, E. C., Gaspelin, N., & Gerhardstein, P. (2022). The development of oculomotor suppression of salient distractors in children. *Journal of Experimental Child Psychology*, 214, 105291. https://doi.org/10.1016/j.jecp.2021.105291

Boas, D. A., Gaudette, T., Strangman, G., Cheng, X., Marota, J. J., & Mandeville, J. B. (2001). The accuracy of near infrared spectroscopy and imaging during focal changes in cerebral hemodynamics. *NeuroImage*, *13*(1), 76–90. https://doi.org/10.1006/nimg.2000.0674

Buss, A. T., & Kerr-German, A. (2019). Dimensional attention as a mechanism of executive function: Integrating flexibility, selectivity, and stability. *Cognition.* https://doi.org/10.1016/j.cognition.2019.06.015

Buss, A. T., & Nikam, B. (2020). Not all labels develop equally: The role of labels in guiding attention to dimensions. *Cognitive Development, 53*, 100843. https://doi.org/10.1016/j.cogdev.2019.100843

Buss, A. T. & Spencer, J. P. (2014). The emergent executive: A dynamic neural field theory of the development of executive function. *Monogr. Soc. Res. Child Dev. 79***,** 1–104.

Cavanna, A. E., & Trimble, M. R. (2006). The precuneus: a review of its functional anatomy and behavioural correlates. *Brain: a journal of neurology*, *129*(Pt 3), 564–583. https://doi.org/10.1093/brain/awl004

Chabal, S., Hayakawa, S., & Marian, V. (2021). How a picture becomes a word: individual differences in the development of language-mediated visual search. *Cognitive research: principles and implications*, *6*(1), 2. https://doi.org/10.1186/s41235-020-00268-9

Chen, G., Adleman, N. E., Saad, Z. S., Leibenluft, E., & Cox, R. W. (2014). Applications of multivariate modeling to neuroimaging group analysis: A comprehensive alternative to univariate general linear model. *NeuroImage (Orlando, Fla.)*, *99*, 571–588. https://doi.org/10.1016/j.neuroimage.2014.06.027

Collins, D. L., Zijdenbos, A. P., Kollokian, V., Sled, J. G., Kabani, N. J., Holmes, C. J., & Evans, A. C. (1998). Design and construction of a realistic digital brain phantom. *IEEE transactions on medical imaging*, *17*(3), 463–468. https://doi.org/10.1109/42.712135

Corbetta, M., & Shulman, G. L. (2002). Control of goal-directed and stimulus-driven attention in the brain. *Nature reviews. Neuroscience*, *3*(3), 201–215. https://doi.org/10.1038/nrn755

Couperus, J. W., & Quirk, C. (2015). Visual search and the N2pc in children. *Attention, Perception, and Psychophysics*, *77*(3), 768–776. https://doi.org/10.3758/s13414-015-0833-5

Cox, R. W. (1996). AFNI: software for analysis and visualization of functional magnetic resonance neuroimages. *Comput Biomed Res 29*(3):162-173. doi:10.1006/cbmr.1996.0014

Cox, R. W., Chen, G., Glen, D. R., Reynolds, R. C., & Taylor, P. A. (2017). FMRI Clustering in AFNI: False-Positive Rates Redux. *Brain Connectivity*, *7*(3), 152–171. https://doi.org/10.1089/brain.2016.0475

Dadario, N. B., & Sughrue, M. E. (2023). The functional role of the precuneus. *Brain : a journal of neurology*, *146*(9), 3598–3607. https://doi.org/10.1093/brain/awad181

Delorme A & Makeig S (2004) EEGLAB: an open-source toolbox for analysis of single-trial EEG dynamics. *Journal of Neuroscience Methods 134*:9-21.

Desai, R.H., Tadimeti, U. & Riccardi, N. (2023). Proper and common names in the semantic system. *Brain Struct Funct*, *228*, 239–254. https://doi-org.utk.idm.oclc.org/10.1007/s00429-022-02593-9

Deveney, C. M., Briggs-Gowan, M. J., Pagliaccio, D., Estabrook, C. R., Zobel, E., Burns, J. L., Norton, E. S., Pine, D. S., Brotman, M. A., Leibenluft, E., & Wakschlag, L. S. (2019). Temporally sensitive neural measures of inhibition in preschool children across a spectrum of irritability. *Developmental Psychobiology*, *61*(2), 216–227. https://doi.org/10.1002/dev.21792

Durston, S., Thomas, K. M., Yang, Y., Uluğ, A. M., Zimmerman, R. D., & Casey, B. J. (2002). A neural basis for the development of inhibitory control. *Developmental Science*, *5*(4), 9–16. https://doi.org/10.1111/1467-7687.00235

Eggebrecht, A. T., & Culver, J. P. (2019). NeuroDOT: an extensible Matlab toolbox for streamlined optical functional mapping. In H. Dehghani & H. Wabnitz (Eds.), *Diffuse Optical Spectroscopy and Imaging VII*, *11074*, 26. SPIE. https://doi.org/10.1117/12.2527164

Fiske, A., & Holmboe, K. (2019). Neural substrates of early executive function development. *In Developmental Review 52*, 42–62. Mosby Inc. https://doi.org/10.1016/j.dr.2019.100866

de Fockert, J., Rees, G., Frith, C., & Lavie, N. (2004). Neural correlates attention capture in visual search. *Journal of Cognitive Neuroscience*, *16*(5), 751–759.

de Fockert, J. W., & Theeuwes, J. (2012). Role of frontal cortex in attentional capture by singleton distractors. *Brain and cognition*, *80*(3), 367-373.

Forbes, S., Wijeakumar, S., Eggebrecht, A., Magnotta, V., & Spencer, J. (2021) Processing pipeline for image reconstructed fNIRS analysis using both MRI templates and individual anatomy. *Neurophotonics 8*(2), 025010. https://doi.org/10.1117/1.NPh.8.2.025010

Gaspelin, N., Leonard, C. J., & Luck, S. J. (2015). Direct Evidence for Active Suppression of Salient-but-Irrelevant Sensory Inputs. *Psychological Science*, *26*(11), 1740–1750. https://doi.org/10.1177/0956797615597913

Gaspelin, N., & Luck, S. J. (2018). Combined Electrophysiological and Behavioral Evidence for the Suppression of Salient Distractors. *Journal of Cognitive Neuroscience*, *30*(9), 1265–1280. https://doi.org/10.1162/jocn_a_01279

Heim, H. R., Lowery, K., Eddings, R., Nikam, B., Kerr-German, A., & Buss, A. T. (2023). Examining Neural Dynamics During Dimensional Label Comprehension and Production as a Function of Dimensional Attention. *Journal of Cognition and Development*, *25*(1), 127–147. https://doi.org/10.1080/15248372.2023.2256859

Hickey, C., McDonald, J. J., & Theeuwes, J. (2006). Electrophysiological Evidence of the Capture of Visual Attention. *Journal of Cognitive Neuroscience*, *18*(4), 604–613. https://doi.org/10.1162/jocn.2006.18.4.604

Huettig, F., Olivers, C. N. L., & Hartsuiker, R. J. (2011). Looking, language, and memory: Bridging research from the visual world and visual search paradigms. *Acta Psychologica, 137*(2), 138–150. https://doi.org/10.1016/j.actpsy.2010.07.013

Huppert, T.J., Diamond, S. G., Franceschini, M. A., & Boas, D. A. (2009). HomER: A review of time-series analysis methods for near-infrared spectroscopy of the brain. *Applied Optics, 48*(10), D280-D298.

Ibbotson, P., & Kearvell-White, J. (2015). Inhibitory control predicts grammatical ability. *PLoS ONE, 10*(12), Article e0145030. https://doi.org/10.1371/journal.pone.0145030

Jaeger, A. (2013). Inhibitory control and the adolescent brain: A review of fMRI research. *Psychology and Neuroscience, 6*(1), 23–30. https://doi.org/10.3922/j.psns.2013.1.05

Katsuki, F., & Constantinidis, C. (2014). Bottom-Up and Top-Down Attention: Different Processes and Overlapping Neural Systems. *The Neuroscientist*, *20*(5), 509–521. https://doi.org/10.1177/1073858413514136

Kerr-German, A. N., & Buss, A. T. (2020). Exploring the Neural Basis of Selective and Flexible Dimensional Attention: An fNIRS Study. *Journal of Cognition and Development*, *21*(3), 313–325. https://doi.org/10.1080/15248372.2020.1760279

Kinder, K. T., Heim, H. L. R., Parker, J., Lowery, K., McCraw, A., Eddings, R. N., Defenderfer, J., Sullivan, J., & Buss, A. T. (2022). Systematic review of fNIRS studies reveals inconsistent chromophore data reporting practices. *Neurophotonics*, *9*(4), 040601. https://doi.org/10.1117/1.NPh.9.4.040601

Kray, J., Kipp, K. H., & Karbach, J. (2009). The development of selective inhibitory control: the influence of verbal labeling. *Acta psychologica*, *130*(1), 48–57. https://doi.org/10.1016/j.actpsy.2008.10.006

Lavie, N., & de Fockert, J. (2006). Frontal control of attentional capture in visual search. *Visual Cognition, 14*(4–8), 863–876. https://doi.org/10.1080/13506280500195953

Liesefeld, H. R., Liesefeld, A. M., Töllner, T., & Müller, H. J. (2017). Attentional capture in visual search: Capture and post-capture dynamics revealed by EEG. *NeuroImage, 156*, 166–173. https://doi.org/10.1016/j.neuroimage.2017.05.016

Liu, Q., Lin, S., Zhao, G., & Roberson, D. (2016). The effect of modulating top-down attention deployment on the N2pc/PCN. *Biological Psychology*, *117*, 187–193. https://doi.org/10.1016/j.biopsycho.2016.04.004

Lowery, K. (2022). Examining Perceptual and Categorical Influences on Visual Working Memory [Unpublished Dissertation]. *University of Tennessee, Knoxville*. https://trace.tennessee.edu/utk_graddiss/7671

Lowery, K., Nikam, B., & Buss, A. T. (2022). Dimensional label learning contributes to the development of executive functions. *Scientific Reports*, *12*(1), 1–12. https://doi.org/10.1038/s41598-022-14761-2

Mani, N., Johnson, E., McQueen, J. M., & Huettig, F. (2013). How yellow is your banana? toddlers' language-mediated visual search in referent-present tasks. *Developmental Psychology*, *49*(6), 1036–1044. https://doi.org/10.1037/a0029382

McCraw, A., Sullivan, J., Lowery, K., Eddings, R., Heim, H. R., & Buss, A. T. (2024). Dynamic field theory of executive function: Identifying early neurocognitive markers. *Monographs of the Society for Research in Child Development*, *89*(3).

Murphy, K., & Fox, M. D. (2017). Towards a consensus regarding global signal regression for resting state functional connectivity MRI. *NeuroImage*, *154*, 169–173. https://doi.org/10.1016/J.NEUROIMAGE.2016.11.052

Pickron, C. B., Iyer, A., Fava, E., & Scott, L. S. (2018). Learning to Individuate: The Specificity of Labels Differentially Impacts Infant Visual Attention. *Child Development*, *89*(3), 698–710. https://doi.org/10.1111/cdev.13004

R Core Team (2023). R: A language and environment for statistical computing. R Foundation for Statistical Computing, Vienna, Austria. https://www.R-project.org/.

Rashal, E., Senoussi, M., Santandrea, E., Ben-Hamed, S., Macaluso, E., Chelazzi, L., & Boehler, C. N. (2022). An EEG study of the combined effects of top-down and bottom-up attentional selection under varying task difficulty. *Psychophysiology*, *59*(6), 1–21. https://doi.org/10.1111/psyp.14002

Rockland, K.S., Graves, W.W. (2023). The angular gyrus: a special issue on its complex anatomy and function. *Brain Struct Funct, 228*, 1–5. https://doi.org/10.1007/s00429-022-02596-6

Sandhofer, C. M., & Smith, L. B. (1999). Learning color words involves learning a system of mappings. *Developmental Psychology, 35*(3), 668–679. https://doi.org/10.1037/0012-1649.35.3.668

Stilwell, B. T., Egeth, H., & Gaspelin, N. (2022). Electrophysiological Evidence for Attentional Suppression of Highly Salient Distractors. *Journal of Vision, 22*(14), 3061-. https://doi.org/10.1167/jov.22.14.3061

Sun, M., Wang, E., Huang, J., Zhao, C., Guo, J., Li, D., Sun, L., Du, B., Ding, Y., & Song, Y. (2018). Attentional selection and suppression in children and adults. *Developmental Science, 21*(6), e12684. https://doi.org/10.1111/desc.12684

Smith, L. B., & Kemler, D. G. (1977). Developmental trends in free classification: Evidence for a new conceptualization of perceptual development. *Journal of*

Experimental Child Psychology, *24*(2), 279–298. https://doi.org/10.1016/0022-0965(77)90007-8

Szczepanski, S. M., Crone, N. E., Kuperman, R. A., Auguste, K. I., Parvizi, J., & Knight, R. T. (2014). Dynamic changes in phase-amplitude coupling facilitate spatial attention control in fronto-parietal cortex. *PLoS biology*, *12*(8), e1001936. https://doi.org/10.1371/journal.pbio.1001936

Tachtsidis, I., & Scholkmann, F. (2016). False positives and false negatives in functional near-infrared spectroscopy: Issues, challenges, and the way forward. *Neurophotonics*, *3*(3), 031405. doi:10.1117/1.NPh.3.3.031405

Theeuwes, J. (1992). Perceptual selectivity for color and form. *Perception & Psychophysics*, *51*(6), 599–606. https://doi.org/10.3758/BF03211656

Theeuwes, J. (2004). Top-down search strategies cannot override attentional capture. *Psychonomic Bulletin and Review*, *11*(1), 65–70. https://doi.org/10.3758/BF03206462

Theeuwes, J. (2010). Top–down and bottom–up control of visual selection. *Acta Psychologica*, *135*(2), 77–99. https://doi.org/10.1016/j.actpsy.2010.02.006

Turoman, N., Tivadar, R. I., Retsa, C., Maillard, A. M., Scerif, G., & Matusz, P. J. (2021). The development of attentional control mechanisms in multisensory environments. *Developmental Cognitive Neuroscience*, *48*, 100930. https://doi.org/10.1016/j.dcn.2021.100930

Vatterott, D. B., Mozer, M. C., & Vecera, S. P. (2018). Rejecting salient distractors: Generalization from experience. *Attention, Perception & Psychophysics*, *80*(2), 485–499. https://doi.org/10.3758/s13414-017-1465-8

Vales, C., & Smith, L. B. (2015). Words, shape, visual search and visual working memory in 3-year-old children. *Developmental science*, *18*(1), 65–79. https://doi.org/10.1111/desc.12179

Wagner, J., & Rusconi, E. (2023). Causal involvement of the left angular gyrus in higher functions as revealed by transcranial magnetic stimulation: a systematic review. *Brain structure & function*, *228*(1), 169–196. https://doi.org/10.1007/s00429-022-02576-w

Wheelock, M. D., Culver, J. P., & Eggebrecht, A. T. (2019). High-density diffuse optical tomography for imaging human brain function. *Review of Scientific Instruments*, *90*(5), 051101. https://doi.org/10.1063/1.5086809

Zelazo, P. D. (2006). The Dimensional Change Card Sort (DCCS): A method of assessing executive function in children. *Nature Protocols*, *1*(1), 297–301. https://doi.org/10.1038/nprot.2006.46

Zhang, J. X., Feng, C. M., Fox, P. T., Gao, J. H., & Tan, L. H. (2004). Is left inferior frontal gyrus a general mechanism for selection?. *NeuroImage*, *23*(2), 596–603. https://doi.org/10.1016/j.neuroimage.2004.06.006

APPENDIX

Table A1. Parameter estimates predicting *right inferior frontal gyrus* activity over levels of RTDiff in the AS paradigm.

Parameter	***b***	***SE b***	***t***	***p***	**95% CI**
HbO	-0.07***	0.02	-4.13	<.001	[-0.11 -0.04]
HbR	0.02	0.02	1.34	.18	[-0.01 0.06]
HbO-HbR	-0.10***	0.03	-3.86	<.001	[-0.14 -0.05]

Note *p<.05, **p<.01, ***p<.001

Table A2.1. Estimated marginal means for hemoglobin across RTDiff levels for the *right inferior frontal gyrus* in the AS paradigm.

RTDiff (ms)	**Parameter**	**ΔHb (μmol/L)**	***SE***	***t***	***p***	**95% CI**
-30	HbO	0.006***	0.001	4.06	<.001	[0.003, 0.009]
	HbR	-0.003	0.001	-1.73	.09	[-0.005, 0.00]
0	HbO	0.004**	0.001	3.23	.001	[0.001, 0.006]
	HbR	-0.002	0.001	-1.57	.12	[-0.004, 0.001]
90	HbO	-0.003	0.002	-1.70	.09	[-0.006, 0.00]
	HbR	0.00	0.002	0.15	.87	[-0.003, 0.003]

Note *p<.05, **p<.01, ***p<.001

Table A2.2. Contrasts for estimated marginal means for hemoglobin across RTDiff levels for the *right inferior frontal gyrus* in the AS paradigm.

RTDiff (ms)	**Contrast**	***b***	***SE b***	***t***	***p***	**95% CI**
-30	HbO-HbR	0.009***	0.002	4.09	<.001	[0.004, 0.013]
0	HbO-HbR	0.006***	0.002	3.40	<.001	[0.002, 0.009]
90	HbO-HbR	-0.002	0.002	-1.31	.19	[-0.007, 0.001]

Note *p<.05, **p<.01, ***p<.001

Table A3. Parameter estimates predicting *left inferior frontal gyrus* activity over levels of RTDiff in the AS paradigm.

Parameter	*b*	*SE b*	*t*	*p*	95% CI
HbO AS Absent	0.05*	0.02	2.01	.046	[0.00, 0.09]
HbR AS Absent	-0.04	0.02	-1.77	.08	[-0.08, 0.00]
HbO AS Present	-0.04	0.02	-1.67	.10	[-0.08, 0.01]
HbR AS Present	0.01	0.02	0.26	.79	[-0.04, 0.05]
HbO AS Absent -HbR AS Absent	0.08*	0.03	2.67	.04	[0.00, 0.17]
HbO AS Present -HbR AS Present	-0.04	0.03	-1.37	.52	[-0.13, 0.04]
HbO AS Absent- HbO AS Present	0.08*	0.03	2.61	.049	[0.00, 0.17]

Note *p<.05, **p<.01, ***p<.001

Table A4. Estimated marginal means for hemoglobin across RTDiff levels for the *left inferior frontal gyrus* in the AS paradigm.

RTDiff (ms)	**Condition**	**Parameter**	**ΔHb (μmol/L)**	***SE***	***t***	***p***	**95% CI**
-30	AS Absent	HbO	-0.005*	0.002	-2.50	.01	[-0.008, -0.001]
		HbR	0.002	0.002	0.78	.44	[-0.002, 0.005]
	AS Present	HbO	0.004*	0.002	2.02	.045	[0.00, 0.008]
		HbR	0.00	0.002	-0.13	.90	[-0.004, 0.004]
0	AS Absent	HbO	-0.003*	0.002	-2.23	.02	[-0.007, 0.00]
		HbR	0.00	0.002	0.19	.84	[-0.002, 0.003]
	AS Present	HbO	0.00	0.002	1.78	.08	[0.00, 0.006]
		HbR	0.00	0.002	-0.04	.97	[-0.003, 0.003]
90	AS Absent	HbO	0.00	0.002	0.33	.74	[-0.003, 0.005]
		HbR	0.00	0.002	-1.66	.10	[-0.007, 0.00]
	AS Present	HbO	0.00	0.002	-0.33	.74	[-0.005, 0.003]
		HbR	0.00	0.002	0.23	.82	[-0.004, 0.004]

Note *p<.05, **p<.01, ***p<.001

Table A5. Contrasts for the estimated marginal means for hemoglobin across RTDiff levels for the *left inferior frontal gyrus* in the AS paradigm.

RTDiff (ms)	**Contrast**	***b***	***SE b***	***t***	***p***	**95% CI**
-30	HbO AS Absent -HbR AS Absent	-0.006	0.003	-2.32	.09	[-0.013, 0.001]
	HbO AS Present -HbR AS Present	0.004	0.003	1.52	.43	[-0.002, 0.011]
	HbO AS Absent- HbO AS Present	-0.008**	0.003	-3.19	.009	[-0.016, -0.002]
0	HbO AS Absent -HbR AS Absent	-0.003	0.002	-1.71	.32	[-0.010, 0.002]
	HbO AS Present -HbR AS Present	0.003	0.002	1.29	.57	[-0.002, 0.009]
	HbO AS Absent- HbO AS Present	-0.006*	0.002	-2.83	.02	[-0.012, 0.001]
90	HbO AS Absent -HbR AS Absent	0.004	0.003	1.40	1.00	[-0.003, 0.011]
	HbO AS Present -HbR AS Present	-0.001	0.003	-0.39	.18	[-0.009, 0.006]
	HbO AS Absent- HbO AS Present	0.001	0.003	0.46	.67	[-0.006, 0.009]

Note *p<.05, **p<.01, ***p<.001

Table A6. Parameter estimates predicting *left inferior parietal lobe* activity over levels of RTDiff in the AS paradigm.

Parameter	***b***	***SE b***	***t***	***p***	**95% CI**
HbO	0.14***	0.04	3.50	<.001	[0.06, 0.22]
HbR	-0.01	0.04	-0.35	.72	[-0.09, 0.06]
HbO-HbR	0.15**	0.06	2.72	0.007	[0.04, 0.26]

Note **p*<.05, ***p*<.01, ****p*<.001

Table A7.1. Estimated marginal means for hemoglobin across RTDiff levels for the left inferior parietal lobe in the AS paradigm.

RTDiff (ms)	**Parameter**	**ΔHb (μmol/L)**	***SE***	***t***	***p***	**95% CI**
-30	HbO	-0.013***	0.004	4.06	<.001	[-0.020, -0.006]
	HbR	0.00	0.004	-1.73	.91	[-0.007, 0.007]
0	HbO	-0.008**	0.002	3.23	.001	[-0.014, -0.004]
	HbR	0.00	0.002	-1.57	.99	[-0.005, 0.005]
90	HbO	0.003	0.003	-1.70	.28	[-0.003, 0.010]
	HbR	-0.001	0.003	0.15	.69	[-0.008, 0.005]

Note *p<.05, **p<.01, ***p<.001

Table A7.2. Contrast for estimated marginal means for hemoglobin across RTDiff levels for the left inferior parietal lobe in the AS paradigm.

RTDiff (ms)	**Contrast**	***b***	***SE b***	***t***	***p***	**95% CI**
-30	HbO-HbR	-0.013**	0.005	-2.72	.008	[-0.023, 0.00]
0	HbO-HbR	-0.009*	0.004	-2.30	.02	[-0.016, -0.001]
90	HbO-HbR	0.005	0.004	1.05	.30	[-0.004, 0.014]

Note *p<.05, **p<.01, ***p<.001

Table A8. Parameter estimates predicting *right angular gyrus* activity over levels of RTDiff in the AS paradigm.

Parameter	***b***	***SE b***	***t***	***p***	**95% CI**
HbO	-0.10*	0.04	-2.55	.01	[-0.17, -0.02]
HbR	0.018	0.04	0.48	.63	[-0.06, 0.09]
HbO-HbR	-0.12*	0.05	-2.14	.03	[-0.22, -0.01]

Note *p<.05, **p<.01, ***p<.001

Table A9.1. Estimated marginal means for hemoglobin across RTDiff levels for the *right angular gyrus* in the AS paradigm.

RTDiff (ms)	**Parameter**	**ΔHb (μmol/L)**	***SE***	***t***	***p***	**95% CI**
-30	HbO	0.012***	0.003	3.64	<.001	[0.005, 0.018]
	HbR	-0.001	0.003	-0.29	.77	[-0.007, 0.005]
0	HbO	0.009***	0.003	3.40	<.001	[0.004, 0.014]
	HbR	0.00	0.003	-0.15	.88	[-0.006, 0.005]
90	HbO	0.00	0.003	0.03	.97	[-0.006, 0.006]
	HbR	0.001	0.003	0.37	.71	[-0.005, 0.008]

Note *$p<.05$, **$p<.01$, ***$p<.001$

Table A9.2. Contrasts for estimated marginal means for hemoglobin across RTDiff levels for the *right angular gyrus* in the AS paradigm.

RTDiff (ms)	**Contrast**	***b***	***SE b***	***t***	***p***	**95% CI**
-30	HbO-HbR	0.012**	0.005	2.78	.006	[0.004, 0.022]
0	HbO-HbR	0.009*	0.004	2.51	.01	[0.002, 0.017]
90	HbO-HbR	-0.001	0.005	-0.24	.81	[-0.011, 0.008]

Note *$p<.05$, **$p<.01$, ***$p<.001$

Table A10. Parameter estimates predicting *left precuneus activity* over levels of RTDiff in the AS paradigm.

Parameter	***b***	***SE b***	***t***	***p***	**95% CI**
HbO	0.06**	0.02	2.87	.005	[0.02, 0.11]
HbR	-0.02	0.02	-0.95	.34	[-0.07, 0.02]
HbO-HbR	0.09**	0.03	2.70	.008	[0.02, 0.14]

Note *p<.05, **p<.01, ***p<.001

Table A11.1. Estimated marginal means for hemoglobin across RTDiff levels for the *left precuneus* in the AS paradigm.

RTDiff (ms)	Parameter	ΔHb (μmol/L)	*SE*	*t*	*p*	95% CI
-30	HbO	-0.004	0.002	-1.86	.07	[-0.008, 0.00]
	HbR	0.001	0.002	0.38	.70	[-0.003, 0.005]
0	HbO	-0.002	0.002	-1.10	.27	[-0.004, 0.001]
	HbR	0.00	0.002	0.07	.94	[-0.003, 0.003]
90	HbO	0.004*	0.002	2.09	.04	[0.00, 0.008]
	HbR	-0.002	0.002	-0.93	.36	[-0.005, 0.002]

Note *p<.05, **p<.01, ***p<.001

Table A11.2. Contrasts for estimated marginal means for hemoglobin across RTDiff levels for the *left precuneus* in the AS paradigm.

RTDiff (ms)	Contrast	*b*	*SE b*	*t*	*p*	95% CI
-30	HbO-HbR	-0.004	0.003	-1.59	.12	[-0.010, 0.001]
0	HbO-HbR	-0.002	0.002	-0.83	.41	[-0.006, 0.003]
90	HbO-HbR	0.006*	0.003	2.13	.04	[0.000, 0.011]

Note *p<.05, **p<.01, ***p<.001

Table A12. Parameter estimates predicting *right superior parietal lobe* activity over levels of RTDiff in the AS paradigm.

Parameter	***b***	***SE b***	***t***	***p***	**95% CI**
HbO AS Absent	-0.04	0.04	-0.86	.39	[-0.12, 0.05]
HbR AS Absent	0.04	0.04	0.84	.40	[-0.05, 0.12]
HbO AS Present	0.11*	0.04	2.50	.01	[0.02, 0.19]
HbR AS Present	-0.04	0.04	-1.03	.31	[-0.13, 0.04]
HbO AS Absent -HbR AS Absent	-0.07	0.06	-1.20	.62	[-0.22, 0.08]
HbO AS Present -HbR AS Present	0.15	0.06	2.49	.07	[-0.01, 0.30]
HbO AS Absent- HbO AS Present	-0.14	0.06	-2.37	.09	[-0.29, 0.01]

Note *p<.05, **p<.01, ***p<.001

Table A13. Estimated marginal means for hemoglobin across RTDiff levels for the *right superior parietal lobe* in the AS paradigm.

RTDiff (ms)	**Condition**	**Parameter**	**ΔHb (μmol/L)**	***SE***	***t***	***p***	**95% CI**
-30	AS Absent	HbO	0.006	0.004	1.77	.08	[0.00, 0.014]
		HbR	0.00	0.004	-0.25	.80	[-0.008, 0.006]
	AS Present	HbO	-0.005	0.004	-1.24	.22	[-0.012, 0.003]
		HbR	0.003	0.004	0.69	.49	[-0.005, 0.010]
0	AS Absent	HbO	0.005	0.003	1.84	.07	[0.00, 0.011]
		HbR	0.00	0.003	0.04	.97	[-0.006, 0.006]
	AS Present	HbO	-0.001	0.003	-0.46	.64	[-0.007, 0.004]
		HbR	0.001	0.003	0.42	.68	[-0.005, 0.007]
90	AS Absent	HbO	0.002	0.004	0.59	.56	[-0.005, 0.009]
		HbR	0.003	0.004	0.89	.37	[-0.004, 0.011]
	AS Present	HbO	0.008*	0.004	2.18	.03	[0.00, 0.015]
		HbR	-0.003	0.004	-0.72	.47	[-0.010, 0.005]

Note *p<.05, **p<.01, ***p<.001

Table A14. Contrasts for the estimated marginal means for hemoglobin across RTDiff levels for the *right superior parietal lobe* in the AS paradigm.

RTDiff (ms)	Contrast	*b*	*SE b*	*t*	*p*	95% CI
-30	HbO AS Absent -HbR AS Absent	0.007	0.005	1.44	.48	[-0.006, 0.021]
	HbO AS Present -HbR AS Present	-0.007	0.005	-1.36	.52	[-0.020, 0.006]
	HbO AS Absent- HbO AS Present	0.011	0.005	2.13	.15	[-0.002, 0.024]
0	HbO AS Absent -HbR AS Absent	0.005	0.004	1.27	.58	[-0.005, 0.016]
	HbO AS Present -HbR AS Present	-0.003	0.004	-0.62	.92	[-0.013, 0.008]
	HbO AS Absent- HbO AS Present	0.007	0.004	1.63	.36	[-0.004, 0.018]
90	HbO AS Absent -HbR AS Absent	-0.001	0.005	-0.21	1.00	[-0.014, 0.012]
	HbO AS Present -HbR AS Present	0.01	0.005	2.05	.18	[-0.003, 0.024]
	HbO AS Absent- HbO AS Present	-0.006	0.005	-1.13	.67	[-0.019, 0.008]

Note **p*<.05, ***p*<.01, ****p*<.001

Table A15. Parameter estimates predicting *right anterior superior parietal lobe* activity over levels of RTDiff in the DLU tasks.

Parameter	*b*	*SE b*	*t*	*p*	95% CI
HbO	-0.45***	0.06	-8.05	<.001	[-0.56, -0.34]
HbR	0.08	0.06	1.37	.17	[-0.03, 0.19]
HbO-HbR	-0.53***	0.08	-6.67	<.001	[-0.69, -0.37]

Note *p<.05, **p<.01, ***p<.001

Table A16.1. Estimated marginal means for hemoglobin across RTDiff levels for the *right anterior superior parietal lobe* in the DLU tasks.

RTDiff (ms)	**Parameter**	**ΔHb (μmol/L)**	***SE***	***t***	***p***	**95% CI**
-30	HbO	0.027***	0.005	5.27	<.001	[0.017, 0.037]
	HbR	-0.004	0.005	-0.78	.43	[-0.014, 0.006]
0	HbO	0.014**	0.004	3.28	.001	[0.005, 0.022]
	HbR	-0.001	0.004	-0.41	.68	[-0.010, 0.006]
90	HbO	-0.027***	0.004	-5.65	<.001	[-0.036, -0.018]
	HbR	0.005	0.004	1.10	.27	[-0.004, 0.015]

Note **p*<.05, ***p*<.01, ****p*<.001

Table A16.2. Contrasts for the estimated marginal means for hemoglobin across RTDiff levels for the *right anterior superior parietal lobe* in the DLU tasks.

RTDiff (ms)	**Contrast**	***b***	***SE b***	***t***	***p***	**95% CI**
-30	HbO-HbR	0.03***	0.01	4.28	<.001	[0.02, 0.05]
0	HbO-HbR	0.02*	0.01	2.61	.01	[0.00, 0.03]
90	HbO-HbR	-0.03***	0.01	-4.77	<.001	[-0.05, -0.02]

Note **p*<.05, ***p*<.01, ****p*<.001

Table A17. Parameter estimates predicting *right posterior superior parietal lobe* activity over levels of RTDiff in the DLU tasks.

Parameter	*b*	*SE b*	*t*	*p*	95% CI
HbO	0.15***	0.04	3.65	<.001	[0.07, 0.23]
HbR	-0.06	0.04	-1.51	.13	[-0.14, 0.02]
HbO-HbR	0.21***	0.06	3.65	<.001	[0.10, 0.32]

Note *p<.05, **p<.01, ***p<.001

Table A18.1. Estimated marginal means for hemoglobin across RTDiff levels for the *right posterior superior parietal lobe* in the DLU tasks.

RTDiff (ms)	**Parameter**	**ΔHb (μmol/L)**	***SE***	***t***	***p***	**95% CI**
-30	HbO	-0.009**	0.003	-2.79	.005	[-0.016, -0.003]
	HbR	-0.001	0.003	-0.34	.72	[-0.008, 0.006]
0	HbO	-0.005	0.003	-1.88	.06	[-0.011, 0.00]
	HbR	-0.003	0.003	-1.10	.27	[-0.008, 0.002]
90	HbO	0.008*	0.004	2.26	.02	[0.001, 0.015]
	HbR	-0.009*	0.004	-2.40	.01	[-0.016, -0.002]

Note *p<.05, **p<.01, ***p<.001

Table A18.2. Contrasts for the estimated marginal means for hemoglobin across RTDiff levels for the *right posterior superior parietal lobe* in the DLU tasks.

RTDiff (ms)	**Contrast**	***b***	***SE b***	***t***	***p***	**95% CI**
-30	HbO-HbR	-0.01	0.01	-1.73	.08	[-0.02, 0.00]
0	HbO-HbR	-0.00	0.00	-0.56	.58	[-0.01, 0.01]
90	HbO-HbR	0.02**	0.01	3.29	.001	[0.01, 0.03]

Note *p<.05, **p<.01, ***p<.001

Table A19. Parameter estimates predicting *right postcentral gyrus* activity over levels of RTDiff in the DLU tasks.

Parameter	***b***	***SE b***	***t***	***p***	**95% CI**
HbO	0.49***	0.09	5.75	<.001	[0.32, 0.66]
HbR	-0.07	0.09	-0.85	.40	[-0.24, 0.10]
HbO-HbR	0.56***	0.12	4.67	<.001	[0.32, 0.80]

Note *p<.05, **p<.01, ***p<.001

Table A20.1. Estimated marginal means for hemoglobin across RTDiff levels for the *right postcentral gyrus* in the DLU tasks.

RTDiff (ms)	**Parameter**	**ΔHb (μmol/L)**	***SE***	***t***	***p***	**95% CI**
-30	HbO	-0.030**	0.009	-3.22	.002	[-0.047, -0.011]
	HbR	0.005	0.009	0.51	.61	[-0.014, 0.023]
0	HbO	-0.015*	0.007	-2.10	.03	[-0.029, -0.001]
	HbR	0.002	0.007	0.35	.73	[-0.012, 0.017]
90	HbO	0.029***	0.005	5.72	<.001	[0.019, 0.039]
	HbR	-0.004	0.005	-0.79	.43	[-0.014, 0.006]

Note *p<.05, **p<.01, ***p<.001

Table A20.2. Contrasts for the estimated marginal means for hemoglobin across RTDiff levels for the *right postcentral gyrus* in the DLU tasks.

RTDiff (ms)	**Contrast**	***b***	***SE b***	***t***	***p***	**95% CI**
-30	HbO-HbR	-0.03*	0.01	-2.64	.01	[-0.06, -0.01]
0	HbO-HbR	-0.02	0.01	-1.73	.08	[-0.04, 0.00]
90	HbO-HbR	0.03***	0.01	4.61	<.001	[0.02, 0.05]

Note *p<.05, **p<.01, ***p<.001

Table A21. Parameter estimates predicting *left middle frontal gyrus* activity over levels of RTDiff in the DLU tasks.

Parameter	***b***	***SE b***	***t***	***p***	**95% CI**
HbO	-0.14	0.03	-5.08	<.001	[-0.20, -0.09]
HbR	0.02	0.03	0.77	.44	[-0.03, 0.08]
HbO-HbR	-0.16	0.04	-4.14	<.001	[-0.24, -0.09]

Note *p<.05, **p<.01, ***p<.001

Table A22.1. Estimated marginal means for hemoglobin across RTDiff levels for the *left middle frontal gyrus* in the DLU tasks.

RTDiff (ms)	**Parameter**	**ΔHb (µmol/L)**	***SE***	***t***	***p***	**95% CI**
-30	HbO	0.00	0.002	0.20	.84	[-0.004, 0.005]
	HbR	0.003	0.002	1.14	.26	[-0.002, 0.008]
0	HbO	-0.004	0.002	-1.92	.06	[-0.008, 0.00]
	HbR	0.003	0.002	1.73	.08	[0.00, 0.007]
90	HbO	-0.016	0.002	-6.71	<.001	[-0.021, -0.012]
	HbR	0.005	0.002	2.17	.03	[0.00, 0.010]

Note **p*<.05, ***p*<.01, ****p*<.001

Table A22.2. Contrasts for the estimated marginal means for hemoglobin across RTDiff levels for the *left middle frontal gyrus* in the DLU tasks.

RTDiff (ms)	**Contrast**	***b***	***SE b***	***t***	***p***	**95% CI**
-30	HbO-HbR	0.00	0.00	-0.66	.51	[-0.01, 0.00]
0	HbO-HbR	-0.01	0.00	-2.58	.01	[-0.01, -0.00]
90	HbO-HbR	-0.02	0.00	-6.27	<.001	[-0.03, -0.02]

Note **p*<.05, ***p*<.01, ****p*<.001

Table A23. Parameter estimates predicting *right middle frontal gyrus* activity over levels of RTDiff in the DLU tasks.

Parameter	***b***	***SE b***	***t***	***p***	**95% CI**
HbO	-0.45	0.05	-8.45	<.001	[-0.55, -0.34]
HbR	0.07	0.05	1.36	.17	[-0.03, 0.18]
HbO-HbR	-0.52	0.07	-6.94	<.001	[-0.67, -0.37]

Note *p<.05, **p<.01, ***p<.001

Table A24.1. Estimated marginal means for hemoglobin across RTDiff levels for the *right middle frontal gyrus* in the DLU tasks.

RTDiff (ms)	**Parameter**	**ΔHb (μmol/L)**	***SE***	***t***	***p***	**95% CI**
-30	HbO	0.024	0.005	5.35	<.001	[0.015, 0.033]
	HbR	-0.007	0.005	-1.60	.11	[-0.016, 0.002]
0	HbO	0.011	0.004	2.96	.003	[0.004, 0.018]
	HbR	-0.005	0.004	-1.39	.16	[-0.012, 0.002]
90	HbO	-0.030	0.005	-6.32	<.001	[-0.039, -0.020]
	HbR	0.001	0.005	0.31	.75	[-0.007, 0.011]

Note **p*<.05, ***p*<.01, ****p*<.001

Table A24.2. Contrasts for the estimated marginal means for hemoglobin across RTDiff levels for the *right middle frontal gyrus* in the DLU tasks.

RTDiff (ms)	**Contrast**	***b***	***SE b***	***t***	***p***	**95% CI**
-30	HbO-HbR	0.03	0.01	4.91	<.001	[0.02, 0.04]
0	HbO-HbR	0.02	0.01	3.08	.002	[0.01, 0.03]
90	HbO-HbR	-0.03	0.01	-4.69	<.001	[-0.04, -0.02]

Note **p*<.05, ***p*<.01, ****p*<.001

Table A25. Parameter estimates predicting *left inferior frontal gyrus* activity over levels of RTDiff in the DLU tasks.

Parameter	***b***	***SE b***	***t***	***p***	**95% CI**
HbO	-0.32	0.04	-7.79	<.001	[-0.40, -0.24]
HbR	0.01	0.04	0.16	.87	[-0.07, 0.09]
HbO-HbR	-0.33	0.06	-5.62	<.001	[-0.44, -0.21]

Note *p<.05, **p<.01, ***p<.001

Table A26.1. Estimated marginal means for hemoglobin across RTDiff levels for the *left inferior frontal gyrus* in the DLU tasks.

RTDiff (ms)	**Parameter**	**ΔHb (μmol/L)**	***SE***	***t***	***p***	**95% CI**
-30	HbO	0.012	0.003	3.57	<.001	[0.006, 0.019]
	HbR	-0.002	0.003	-0.69	.49	[-0.009, 0.004]
0	HbO	0.003	0.003	1.03	.31	[-0.003, 0.008]
	HbR	-0.002	0.003	-0.79	.43	[-0.008, 0.003]
90	HbO	-0.026	0.004	-7.15	<.001	[-0.033, -0.019]
	HbR	-0.002	0.004	-0.45	.65	[-0.009, 0.005]

Note **p*<.05, ***p*<.01, ****p*<.001

Table A26.2. Contrasts for the estimated marginal means for hemoglobin across RTDiff levels for the *left inferior frontal gyrus* in the DLU tasks.

RTDiff (ms)	**Contrast**	***b***	***SE b***	***t***	***p***	**95% CI**
-30	HbO-HbR	0.01	0.005	3.01	.002	[0.01, 0.02]
0	HbO-HbR	0.01	0.004	1.29	.20	[0.00, 0.01]
90	HbO-HbR	-0.02	0.005	-4.74	<.001	[-0.03, -0.01]

Note **p*<.05, ***p*<.01, ****p*<.001

VITA

Hollis Lee Ratliff Heim was born and raised in Amarillo, Texas to Sunny Horton Ratliff and Franklin Xaver Ratliff. She graduated from Tascosa High School in 2016 and the University of Texas at Dallas, *magna cum laude*, in 2019 with a Bachelor of Science in Neuroscience and a minor in Child Learning and Development. Following graduation, Hollis began her graduate program in Experimental Psychology at the University of Tennessee, Knoxville with a Cognitive and Developmental Science concentration. Under the supervision of Dr. Aaron T. Buss, she graduated from the University of Tennessee, Knoxville in 2021 with a Master of Arts in Experimental Psychology with a thesis titled, "Neural activation during dimensional label learning predicts dimensional attention". Her research focuses on the development of attention and inhibition in children. After graduation, Hollis will continue her work in the field of Child Psychology and continue her passion of teaching in higher education.